
MEASURING THE SEVERITY OF MULTI-COLLINEARITY IN HIGH DIMENSIONS

A PREPRINT

✉ **Wei Q. Deng**

Department of Psychiatry and Behavioural Neurosciences
McMaster University
Peter Boris Centre for Addictions Research
St. Joseph's Healthcare Hamilton
Hamilton, Canada
dengwq@mcmaster.ca

Radu V. Craiu

Department of Statistical Sciences
University of Toronto
Toronto, Canada
radu.craiu@utoronto.ca

✉ **Lei Sun**

Department of Statistical Sciences
Dalla Lana School of Public Health
University of Toronto
Toronto, Canada
sun@utstat.toronto.edu

March 22, 2022

ABSTRACT

Multi-collinearity is a wide-spread phenomenon in modern statistical applications and when ignored, can negatively impact model selection and statistical inference. Classic tools and measures that were developed for “ $n > p$ ” data are not applicable nor interpretable in the high-dimensional regime. Here we propose 1) new individualized measures that can be used to visualize patterns of multi-collinearity, and subsequently 2) global measures to assess the overall burden of multi-collinearity without limiting the observed data dimensions. We applied these measures to genomic applications to investigate patterns of multi-collinearity in genetic variations across individuals with diverse ancestral backgrounds. The measures were able to visually distinguish genomic regions of excessive multi-collinearity and contrast the level of multi-collinearity between different continental populations.

Keywords genomic data · high-dimensional · multi-collinearity

1 Introduction

In the current age of information, statisticians often benefit from the ubiquitous capacity to measure multiple features or covariates for each unit in a sample. For example, large-scale genomic analyses typically measure tens of millions genetic features for tens of thousands of samples and proteomic assay can characterize thousands of circulating proteins for hundreds of individuals [Suhre et al., 2021]. A somewhat reversal of this fortune occurs when the number of units n does not keep pace with the number of features p , thus leading to the high-dimensional data matrices $X \in R^{n \times p}$ for which $n < p$ [Donoho et al., 2000]. For such data, the multi-collinearity phenomenon, in which one feature vector is highly correlated to linear combinations of the remaining ones, is inevitable and often produces damaging effects on model selection and statistical inference [Fan and Lv, 2008]. However, assessing the severity of multi-collinearity in high dimensions is not straightforward as such a measure must factor in both the number of variables involved as well as the degree of collinearity among variables. The absence of a severity measure in high-dimensional settings seems disconnected from the fact that variable selection remains pivotal in balancing model accuracy and interpretability

[George, 2000, Wasserman and Roeder, 2009]. Moreover, identifying which covariates are correlated or even redundant can be as important as finding a subset with high explanatory power.

There are some potential candidates for measuring multi-collinearity in high dimensions. The *Red* indicator [Kovács et al., 2005] has been proposed to quantify the average level of correlation in the data. An almost identical quantity is the root mean square correlation over all $p(p-1)/2$ pairs variables introduced in Efron [2010], also a key component in the approximation of covariance. These are single number measures that do not point to any specific variables, but cast light on the appropriate next-steps. For example, they can guide the implementation of regularization or penalization techniques in the context of high-dimensional linear regression, such as least absolute shrinkage and selection operator (lasso; Santosa and Symes, 1986, Tibshirani, 1996) or elastic net regularization [Zou and Hastie, 2005].

We can perhaps learn from the more accessible scenario of $n > p$, where diagnostic measures to assess severity of multi-collinearity have been reliably used, especially in the context of linear regression [Farrar and Glauber, 1967, Marquardt, 1970, Belsley, 2014]. These measures fall into two categories, one relying on a collection of numbers measuring the impact or burden of multi-collinearity on each individual variable, and the other category that uses a single number to summarize the severity of multi-collinearity of all variables or a subset of the variables.

Examples of the former include a class of measures that incorporate various functions of the estimated coefficient of determination R_j^2 from linear regression models. In essence, this type of measure leverages information on how well the j th variable is explained by linear combinations of the others as an indicator of the severity of collinearity. Among them, the most commonly used is the variance inflation factor (*VIF*; Marquardt, 1970), defined by

$$VIF_j = \frac{1}{1 - R_j^2},$$

intuitively interpreted as the inflating factor for the variance of the estimated regression coefficient for the j th variable. *VIF* not only captures the degree of multi-collinearity for each variable, but also illustrates a direct impact on inference in linear regression models [Fox, 1984]. Departing from examining X alone for multi-collinearity, a corrected *VIF* (denoted *CVIF*; Curto and Pinto, 2011) was proposed to differentiate variables based on whether the redundant information is predictive of the response variable or not. The corrected *CVIF* is preferred over *VIF* when the redundancy among variables is unrelated to the response variable [Curto and Pinto, 2011]. These individual-valued measures offer a mechanism to remove variables implicated in near or perfect multi-collinearity according to a pre-defined threshold (e.g. VIF_j or $CVIF_j > 10$), and thus ensure coefficient estimates of the remaining variables using ordinary least square (OLS) are numerically stable.

The second class of measures uses a single number to summarize multi-collinearity. The most notable being the condition number, defined by the ratio of the largest and smallest singular values of a data matrix [Rice, 1966, Geurts, 1982]. It is directly related to the matrix solution of a linear system and describes the degree to which the matrix $X^T X$ is ill-conditioned. For a scaled data matrix with unit variance in each column, a value between 15 and 30 is considered moderately problematic and severe if above 100 [Belsley et al., 2005]. Closely related is the condition index [Belsley, 2014], which is defined by the square root of ratio of the largest eigenvalue and each of the remaining eigenvalue of $X^T X$. The number of condition indices above a threshold further indicates the number of near or perfect multi-collinear relationships in the data. Other global measures include those examining the determinant of $X^T X$, such as the Farrar-Glauber test statistic [Farrar and Glauber, 1967] that evaluates a function of the determinant of $X^T X$.

In practice, application of the two classes of measures need not be mutually exclusive. In fact, it has been shown that *VIF*s are bounded above by the squared condition number [Berk, 1977, Salmerón et al., 2018], implying that there could be additional information in condition number that is not captured by *VIF*s. Indeed, sometimes problematic variables are restricted to a particular subset while their individual *VIF*s might not all be strong enough to be picked up at the recommended threshold. A generalization of the *VIF* has been proposed by Fox and Monette [1992] to measure an arbitrary subset of variables for evidence of multi-collinearity, which can be used to identify specific sources of imprecision.

Under $n < p$, measures such as *VIF* cannot be reliably calculated, while overall measures that rely on the sample eigenvalues or singular values could be misleading, as we demonstrate in Section 3.2. Further, the usual approach to visualize pairwise relationship quickly becomes cumbersome as the number of combinations increases exponentially. Finally, though the *Red* indicator or the root mean square correlation can be useful as an overall summary, they do not fully address the complexity of multi-collinearity in high-dimensional settings.

This paper contributes in two new ways to the study of multi-collinearity in the case of high-dimensional data. First, it introduces new measures for the severity of multi-collinearity derived via the singular value decomposition (SVD) of X . Second, it uses these novel measures to establish whether the multi-collinearity is due to all or just a few of the variables. The remaining paper is organized as follows. Section 2 introduces the individual-valued measures, presents their empirical properties, and motivates an overall summary measure. Section 3 illustrates the utility of these measures

to visualize and characterize multi-collinearity, making them an attractive option for exploratory data analysis on high-dimensional data. Section 4 demonstrates their application to genotype data from the 1000 Genomes Project [1000 Genomes Project Consortium and others, 2015] to learn about the different patterns of multi-collinearity in genetic variations arising from diverse ancestral backgrounds.

2 A severity measure of multi-collinearity

Let $X \in \mathbb{R}^{n \times p}$ be the observed data matrix with each column standardized to have sample mean 0 and variance 1. We are interested in the high-dimensional data setting ($n < p$) that is the signature of large-scale data such as those arising from genomic applications, but results also naturally generalize to the data rich setting ($n > p$). Denote the SVD of X by UDV^T , where columns of $U \in \mathbb{R}^{n \times (n-1)}$ are the left singular vectors, D is a diagonal matrix with singular values $d_1 \geq d_2 \geq \dots \geq d_{n-1} \geq 0$, and columns of $V \in \mathbb{R}^{p \times (n-1)}$ are the right singular vectors. The column standardization results in the loss of one degree of freedom such that $\sum_{i'=1}^{n-1} d_{i'}^2 = (n-1)p$, which is the sum of the main diagonal elements of $X^T X \in \mathbb{R}^{p \times p}$. Notice that by permitting $d_{i'} = 0$, the matrix X is allowed to be rank deficient, which would be the consequence of perfect collinearity involving two or more variables.

Define the *right severity* measure of multi-collinearity by

$$SR_j = V_{j.} D^4 V_{j.}^T = \sum_{i'=1}^{n-1} v_{ji'}^2 d_{i'}^4,$$

where $V_{j.}$ denotes the j th row and $v_{ji'}$ the (j, i') th entry of V .

Naturally, the duality of SVD allows the definition a *left severity*:

$$SL_i = U_{i.} D^4 U_{i.}^T = \sum_{i'=1}^{n-1} u_{ii'}^2 d_{i'}^4,$$

where $U_{i.}$ denotes the i th row and $u_{ii'}$ the (i, i') th entry of U .

Notice that these two measures are equal when X is symmetric (i.e. $X = X^T$). Both SR and SL leverage the spectrum of singular values of X , similar to other measures of multi-collinearity, but also the singular vectors, which are used to assign a value to each variable/sample through the weighted l_2 norm of the corresponding right/left singular vector. In this construction, the singular values comprehensively capture the variance spectrum, and weighting by their respective singular vectors creates individualized measures irrespective of the data dimensions. Since the top singular values bear the higher burden of capturing the variance in $X^T X$ and contribute more weight to the measures, SL_i and SR_j are termed the univariate burden of variance adjustment (uBVA) measure for left and right severity, respectively.

2.1 Basic properties

Without invoking any distributional or data dimensions assumptions, we first establish three basic properties of $\{SR_j\}_{j=1, \dots, p}$ given any observed $X \in \mathbb{R}^{n \times p}$ with each column standardized to have sample mean 0 and variance 1.

Property 2.1.

$$\sum_{j=1}^p SR_j = \sum_{i=1}^n SL_i = \sum_{i'=1}^{n-1} d_{i'}^4 \quad (2.1)$$

Remark 2.1. Though the sums of SR_j and SL_i are the same, the collective pattern of these values is influenced by the underlying column and row dependence, respectively.

Property 2.2.

$$SR_j = \sum_{i'=1}^{n-1} v_{ji'}^2 d_{i'}^4 = (n-1)^2 \sum_{j'=1}^p r_{jj'}^2, \quad (2.2)$$

where $r_{jj'}$ denotes the sample Pearson's correlation coefficient between the j th and j' th columns. Note that since the data had been column-standardized, we have $r_{jj}^2 = 1$ for all $j = 1, \dots, p$.

Remark 2.2. The equivalent expression of SR_j , shown in equation (2.2), offers some intuition to the construction of the measure. The magnitude of SR_j scales with the variance of the j th column itself as well as any redundancy due to its correlation with all other columns. The larger SR_j is, the more the j th column is involved in multi-collinearity, quantified by the number and severity of these collinear relationships.

Remark 2.3. Since $r_{jj'}^2 \in [0, 1]$, the maximum value of SR_j is bounded by $(n-1)^2 p$, while the minimum possible value is bounded by $(n-1)^2$. These bounds apply to any $X \in \mathbb{R}^{n \times p}$, irrespective of $n > p$ or $n < p$. However, a tighter bound is established in the next property when we restrict data dimensions to be $n < p$.

Property 2.3. When $n < p$,

$$SR_j \in \left[\frac{(n-1)^2}{\sum_{i'=1}^{n-1} v_{ji'}^2}, d_1^2(n-1) \right].$$

Remark 2.4. When $n > p$, the lower bound becomes $(n-1)^2$ assuming all p columns are mutually orthogonal. However, when $n < p$, X has at most $\min(n, p) - 1$ orthogonal columns; the restriction of dimension ($n < p$) leads to a tighter lower bound than $(n-1)^2$ because the squared row norm of a column orthogonal matrix is strictly less than 1 (i.e. $\sum_{i'=1}^{n-1} v_{ji'}^2 < 1$). In fact, following from $\sum_{j=1}^p \sum_{i'=1}^{n-1} v_{ji'}^2 = n-1$, the lower bound $\frac{(n-1)^2}{\sum_{i'=1}^{n-1} v_{ji'}^2}$ is expected to vary for each j , but the smallest such lower bound is strictly smaller than $(n-1)p$. In other words, the smallest value SR_j can take under a high-dimensional data setting is greater than that under the one with $n > p$, the result of spurious correlation as discussed in Fan et al. [2012]. Clearly, the severity increases with an increasing p/n ratio. Meanwhile, as $\sum_{i'=1}^{n-1} d_{i'}^2 = (n-1)p$, the upper bound $d_1^2(n-1)$ is also bounded above by the naive upper bound of $(n-1)^2 p$, but these two are equivalent when columns of X are identical and $\sum_{i'=1}^{n-1} d_{i'}^2 = d_1^2$.

Remark 2.5. Under column standardization, the bounds of SL_i are not directly informative as the singular values are scaled to have unit column variance. Thus, we provide bounds for SL_i assuming row standardization and $n < p$, which implies that $\sum_{i'=1}^{n-1} d_{i'}^2 = n(p-1)$ and $\sum_{i'=1}^{n-1} u_{ii'}^2 d_{i'}^2 = p-1$. The upper bound is then:

$$SL_i = \sum_{i'=1}^{n-1} u_{ii'}^2 d_{i'}^4 \leq d_1^2 \sum_{i'=1}^{n-1} u_{ii'}^2 d_{i'}^2 \leq d_1^2(p-1),$$

and the lower bound follows from the Cauchy-Schwarz inequality:

$$SL_i = \sum_{i'=1}^{n-1} u_{ii'}^2 d_{i'}^4 \geq \left(\sum_{i'=1}^{n-1} u_{ii'}^2 \right) \left(\sum_{i'=1}^{n-1} u_{ii'}^2 d_{i'}^2 \right)^2 \geq (p-1)^2.$$

Thus far, we have not invoked any distributional assumptions. By assuming each row of X follows a multivariate normal distribution, the expected value of SR_j can be expressed in terms of the true covariance matrix and data dimensions when $n > p-1$.

Lemma 2.1. Suppose rows of $X \in \mathbb{R}^{n \times p}$ are independent and identically distributed (i.i.d) normal random vectors, i.e. for $i \in \{1, \dots, n\}$, $x_i \sim \mathcal{N}(0, \Sigma)$, where Σ is positive definite with rank p and Σ_j is the j column of Σ , then

$$E(SR_j) = (n-1)\Sigma_{jj} \text{tr}(\Sigma) + n(n-1)\Sigma_j^T \Sigma_j.$$

This result suggests that the expected value of the proposed measure SR_j has two components, one that is driven by data dimensions (n and p) and the other by the non-zero off-diagonal entries in the corresponding columns of Σ .

Remark 2.6. The above result does not apply to the $n < p$ setting as the scaled sample covariance $X^T X$ no longer follows a Wishart distribution due to the insufficient degrees of freedom [Wishart, 1928]. In this case, $X^T X$ is said to have a singular Wishart distribution and explicit moments are not available [Srivastava, 2003]. An alternative solution is to consider a low-rank approximation of $X^T X$ with rank r ($r < n$) and compute the approximated expectation, at the cost of slightly underestimating $E(SR_j)$.

Though the main focus here was on the empirical properties of these measures without distributional assumptions, it is possible to further characterize the statistical properties of SR_j or SL_i according to behaviours of the singular values and vectors using random matrix theory such as in Bai [2008]. This will be the subject of future work.

Following property 2.2, it is natural to define a scaled measure:

$$sR_j = \frac{SR_j}{(n-1)^2} = \sum_{j'=1}^p r_{jj'}^2 \in [1, p], \quad (2.3)$$

as it has a more natural interpretation of being the sum of squared pairwise Pearson's correlation coefficients. From the row perspective, sL_i can also be defined similarly, provided the data had been row standardized:

$$sL_i = \frac{SL_i}{(p-1)^2} \in [1, n]. \quad (2.4)$$

As the results in Section 2.1 can be conveniently expressed by a rescaling, the bounds on sR_j become:

$$sR_j \in \left[\frac{1}{\sum_{i'=1}^{n-1} v_{ji'}^2}, \frac{d_1^2}{n-1} \right], \quad (2.5)$$

where $\frac{1}{\sum_{i'=1}^{n-1} v_{ji'}^2} \leq 1$, taking equality when $n > p$; and $\frac{d_1^2}{n-1} \leq p$, taking equality when all columns are identical (i.e. $\sum_{i'=1}^{n-1} d_{i'}^2 = d_1^2 = (n-1)p$). The upper and lower bounds are expected to be numerically close when multi-collinearity is driven by spurious correlation due to $n < p$ alone, but further apart as both the number and strength of multi-collinear relationships increase.

The result in Lemma 2.1 becomes:

$$E(sR_j) = \frac{p}{n-1} + \frac{n}{n-1} \Sigma_j^T \Sigma_j, \quad (2.6)$$

which reveals the direct impact of relative data dimensions, $p/(n-1)$, on the severity of multi-collinearity.

2.2 sRs: a unifying measure of multi-collinearity

Since $\{sR_j\}$ is considered the individualized measure of multi-collinearity, we propose a summary measure sRs as a weighted sum of sR_j with two components:

$$sRs = \frac{\sum_{j=1}^p sR_j - p}{p(p-1)} \times \frac{w_1 + w_2}{2} + \frac{\sum_{j=1}^p sR_j - p}{p[d_1^2(n-1)^{-1} - 1]} \times \left(1 - \frac{w_1 + w_2}{2}\right) \in [0, 1], \quad (2.7)$$

where

$$w_1 = \frac{\sum_{d_i^2 > p} d_i^2}{\sum d_i^2}$$

adjusts the weight of ‘bulk’ behaviour more heavily when $n < p$ and

$$w_2 = \frac{\sum_{d_i^2 > (\sqrt{n} - \sqrt{p})^2} d_i^{-2}}{\sum d_i^{-2}},$$

so that $1 - w_2$ adjusts the weight of ‘local’ behaviour more pronouncedly when $n > p$.

We refer to the first component in (2.7) as bulk sRs ($BsRs$):

$$BsRs = \frac{\sum_{j=1}^p sR_j - p}{p(p-1)}, \quad (2.8)$$

which captures the overall burden of multi-collinearity, weighted by the proportion of singular values exceeding their averaged value (maximum of n or p). The second component in (2.7) is designed specifically to account for the number of ‘locally’ strong relationships and defined as local sRs ($LsRs$):

$$LsRs = \frac{\sum_{j=1}^p sR_j - p}{p[d_1^2(n-1)^{-1} - 1]}. \quad (2.9)$$

Notice that, p is used as the upper bound for sR_j when the ‘bulk’ behaviour dominates, i.e. the majority of variance is in the leading singular values, while the maximum given by (2.5) is used when the top singular values do not dominate others. In other words, the combined measure includes each sR_j but weighs the signal relatively.

The sRs ‘bulk’ component is mathematically equivalent to the squared *Red*, defined as

$$\text{Red} = \sqrt{\frac{\text{tr}[X^T X X^T X - (n-1)^2 I_p]}{p(p-1)(n-1)^2}}, \quad (2.10)$$

and both describe the ‘average correlation’ of all variables. But the addition of a ‘local component’ in sRs helps account for strong ‘local’ collinearity that involves only a subset of the variables.

The lower bound of $sRs = 0$ is achieved when $n > p$ and columns of X are mutually orthogonal; the upper bound of $sRs = 1$ is achieved when columns of X are identical. Our proposed sRs , along with $LsRs$ and $BsRs$, have better interpretation as compared to the *Red* indicator, e.g. a value closer to 0 suggests no evidence of multi-collinearity. In contrast, a value closer to 1 indicates severe multi-collinearity due to 1) a subset of variables (local), a scenario that *Red* was unable to capture; 2) a large number of variables (bulk); 3) both 1) and 2). The relative contribution of $LsRs$ and $BsRs$ to sRs can be used to suggest which one of the scenarios constitutes the main driver of observed multi-collinearity.

3 On the use of right severity measure for data exploratory analysis

This section focuses on the utility of sR_j and sRs ($LsRs$ and $BsRs$) through simulation studies. In section 3.1, we applied sR_j to high-dimensional data simulated under different covariance structures to confirm basic properties of sR_j and to explore its use for initial data analysis. In Section 3.2, we compared sRs ($LsRs$ and $BsRs$) with existing measures to assess multi-collinearity in data generated under various multi-collinearity patterns assuming either a high-dimensional ($n < p$) or data rich scenario ($n > p$).

3.1 Visualizing data covariance structure

As each sR_j is a weighted sum of singular values and that the spectrum of singular values is driven by the covariance structure from which the data were sampled, it is tempting to use $\{sR_j\}_{j=1,\dots,p}$ to identify certain “signatures” in the sample covariance through a visual inspection. Property 2.2 (i.e. $sR_j = \sum_{j'=1}^p r_{jj'}^2$), suggests that the observed range of $\{sR_j\}_{j=1,\dots,p}$ is directly related to the number and strength of squared pairwise correlation coefficients. While Property 2.3 implies that the observed extremes of $\{sR_j\}_{j=1,\dots,p}$ are specific to the data beyond dimensions. In summary, the observed patterns of sR_j are reflective of the singular values and can be visualized to give a fuller picture of the covariance structure.

With simulated examples, we demonstrate the usefulness of this measure to differentiate some representative covariance structures. The data dimensions were fixed at $n = 500$ and $p = 1,000$. Following the standard notation, we use J_p to denote an $p \times p$ matrix of ones and I_p a $p \times p$ identity matrix. Each row of X was generated according to $x_i \sim \mathcal{N}(0, \Sigma)$, where

- A. $\Sigma = I_p$ denotes a case of identity covariance,
- B. $\Sigma = J_p\rho + (1 - \rho)I_p$, a compound symmetric structure with $\rho = 0.2$,
- C. $\Sigma_{i,j} = \rho^{|j-i|}$, a first order autoregressive (AR1) structure with $\rho = 0.8$.
- D. $\Sigma = \text{diag}[(0.1 \times J_{p/2} + 0.9I_{p/2}), (0.4 \times J_{p/4} + 0.6I_{p/4}), (0.6 \times 1_{p/4} + 0.4I_{p/4})]$, a covariance with three compound symmetric blocks,
- E. $\Sigma = LL^T + \zeta^2 I_p$, a spiked covariance with two distinct eigenvalues; the low-rank representation $L = V_{1:k}O$ is given by the first k columns of the right singular vectors, $k = 10$, $O = \frac{1}{\sqrt{n}} \text{diag}[\sqrt{10}, \dots, \sqrt{10}]$, and $\zeta^2 = 0.4$,
- F. $\Sigma = LL^T + \zeta^2 I_p$, a spiked covariance with $k + 1$ distinct eigenvalues; $k = 10$, $O = [o_1, \dots, o_k]$, where $o_k^2 = 2 + \zeta^2$ and $\zeta^2 = 0.4$.

For the spiked covariance models, when O is not given explicitly, we assumed o_1^2, \dots, o_{k-1}^2 follow an exponential decay, which uniquely determined the values via the constraints imposed by $o_k^2 = 1 + \zeta^2$ and $\sum_{i=1}^k o_i^2 + p\zeta^2 = p$.

The sample eigenvalues (or normalized squared singular values) shown in Figure 1 (A-F) have distinct patterns under each structure: a relatively smooth decay in the case of an identity covariance (A) and AR1 structure (C); a sharp drop is identified for the compound symmetry case (B), the block-wise compound symmetric covariance (D), and the spiked covariance with two identical true eigenvalues (E); and finally a visible “elbow” for the spiked covariance with $k + 1$ unique true eigenvalues (F). However, these might not be sufficient to differentiate the block-diagonal and the low-rank spiked covariance cases. This is where $\{sR_j\}$ could lend additional information.

The identity case (Figure 1-A) is equivalent to each entry having a standard normal distribution and Marchenko-Pastur law [Marchenko and Pastur, 1967] applies. We expected the observed sR_j and sL_i to fall between $(\frac{p}{n}, (1 + \sqrt{n/p})^2 \frac{p}{n})$ and $(1, \frac{d_1^2}{p})$, which translate to $(2.00, 5.83)$ and $(1.00, 2.91)$, respectively. These are consistent with the observed ranges of $(2.72, 3.31)$ for sR_j and $(1.15, 1.81)$ for sL_i (Figure 1-A). The observed sR_j had a tight symmetrical shape, with most values centred around its observed median (3.005), which was approximately the same as its observed mean (3.007).

The sample eigenvalues of an AR1 structure (Figure 1-C) behaved similarly to that of an identity covariance with the additional variance for each principal direction contributed by only nearby variables. The empirical pattern should also be unimodal and symmetric around its mean/median, but differ in the extremes from the identity case. In practice, for large p , the majority of sR_j should have expected values close or equal to the maximum because $\rho^{|j-i|}$ diminishes quickly as $|j-i|$ increases. For fixed data dimensions, the observed range of $(3.65, 5.70)$ was attributed to the parameter value $\rho = 0.3$. As ρ increases, the range will become wider with a smaller minimum and a larger maximum.

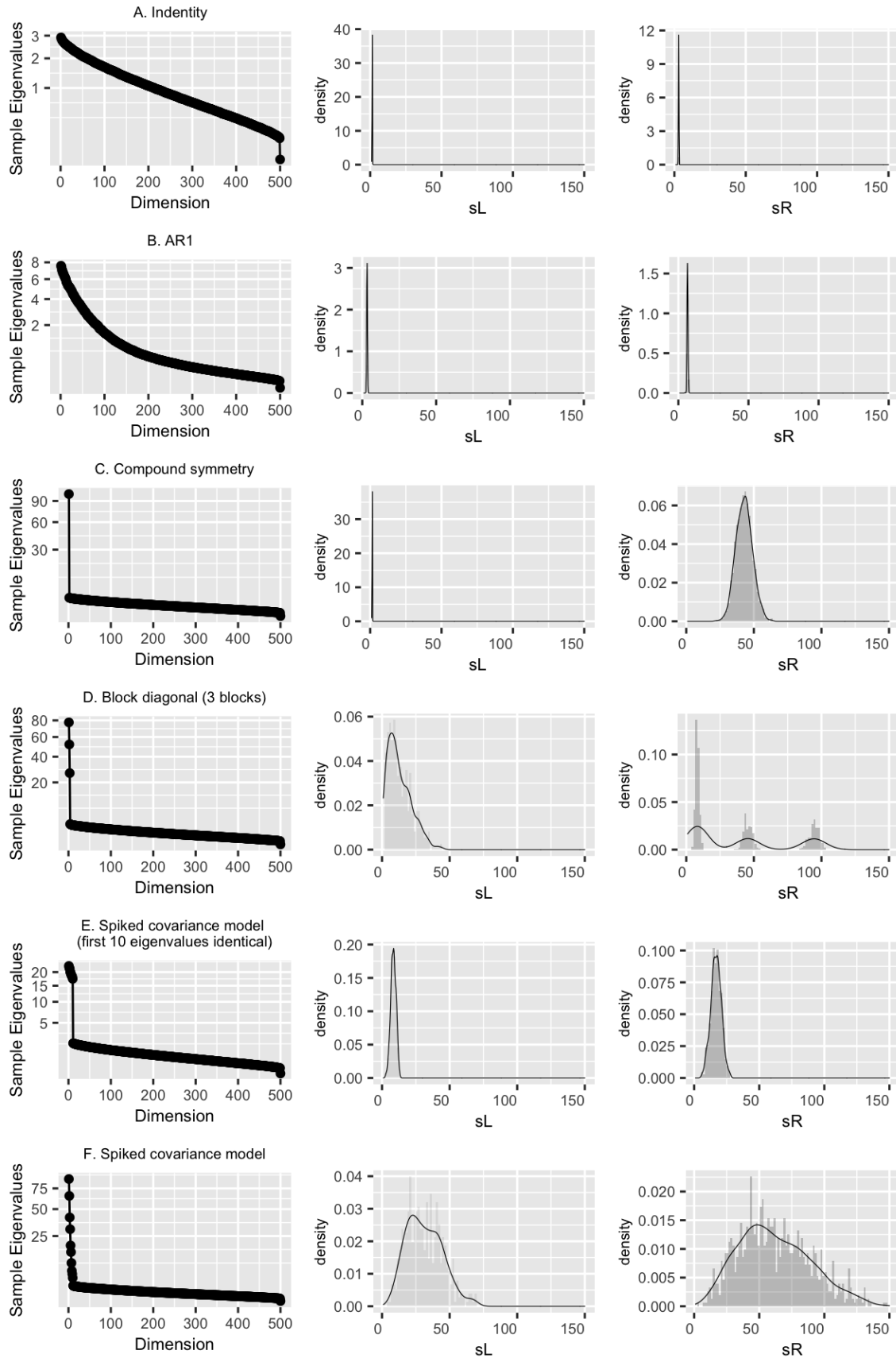


Figure 1: Empirical distributions of sample eigenvalues, sL_i and sR_j under different data covariance structures.

When the true covariance matrix $\Sigma = (1 - \rho)I_p + 1_p\rho$ has a compound symmetric structure (Figure 1-B), the largest population singular value is $\sqrt{n[1 + (p - 1)\rho]}$ and the remaining $n - 1$ singular values are $\sqrt{(1 - \rho)(p - 1)}$. For small ρ values, sR_j is influenced mostly by the top singular values and their corresponding singular vectors. Since all pairwise variables have the same 2×2 covariance, as expected, the empirical distribution of sR_j was roughly symmetric with a unimodal shape that peaked around the mean (42.84) and median (42.81).

When Σ exhibits a block structure and each block is compound symmetric:

$$\Sigma = \begin{bmatrix} \Sigma_1 & 0 & 0 \\ 0 & \Sigma_2 & 0 \\ 0 & 0 & \Sigma_3 \end{bmatrix},$$

the empirical patterns of $\{sR_j\}_j$ should feature three visible modes corresponding to each block similarly described for a compound symmetric structure (Figure 1-D). However, note that if any two blocks are identical, sR_j would simply be duplicated for the identically distributed variables in these two blocks. As a result, two of the three modes would completely overlap, forming a single mode. In general, the number of modes corresponding to the number of unique blocks while the within block pattern depends on the structure of that block.

The last scenario focused on variables with varying magnitudes of pairwise correlation such that the true covariance followed a spiked structure whereby $\Sigma = VO^2V^T + \zeta^2I_p$ (Figure 1-E,F). Though challenging to estimate sample covariance directly, the empirical patterns of sR_j was mostly be driven by the top singular values whose true values are proportional to diagonal elements of V . As a result, the empirical patterns spread much wider (ranging from 8.13 to 138.43) and no modes would be unambiguously identified unless the top singular values were truly identical. Indeed, when the true covariance has equal eigenvalues, the observed $\{sR_j\}$ (ranging from 5.76 to 30.26) can be made to resemble a compound symmetry covariance by varying the two unique eigenvalues. Nevertheless, it can be argued that the compound symmetry covariance is actually a special case of a spiked covariance model with only one spike.

3.2 Measuring the severity of multi-collinearity

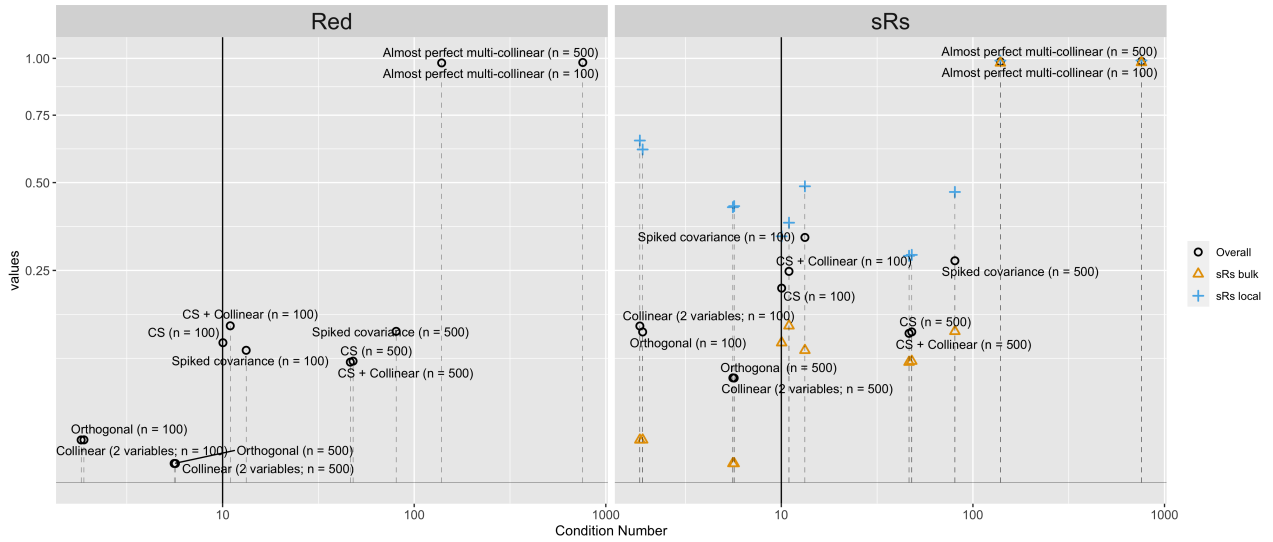
We have proposed $\{sR_j\}$ and sRs as individual-valued and summary-level measures, respectively, to assess severity of multi-collinearity in high dimensions where existing measures fall short. Here we benchmark their performance against alternatives under high-dimensional settings ($n < p$) and data rich settings ($n > p$). Sample size of the simulated data was varied ($n = 100$ and $n = 500$), and the number of variables was fixed at $p = 1,000$ for the high-dimensional or $p = 50$ for the data rich scenarios.

In contrast to the previous simulation study of general covariance structures, we specified covariance matrix to represent no multi-collinearity via an identity matrix (orthogonal design), multi-collinearity through two near-collinear variables (collinear), a moderate level of multi-collinearity impacting all variables through a compound-symmetric covariance matrix (CS), a severe multi-collinearity impacting all variables through a spiked covariance model (spiked covariance), and the most severe case of nearly all variables are identical (almost perfect multi-collinear). To make a more interesting comparison, we also included a block-wise scenario where two variables are near-collinear but the remaining variables follow a compound-symmetric covariance structure. Similar to the simulations in Section 3.1, each row of X was generated according to $x_i \sim \mathcal{N}(0, \Sigma)$, where

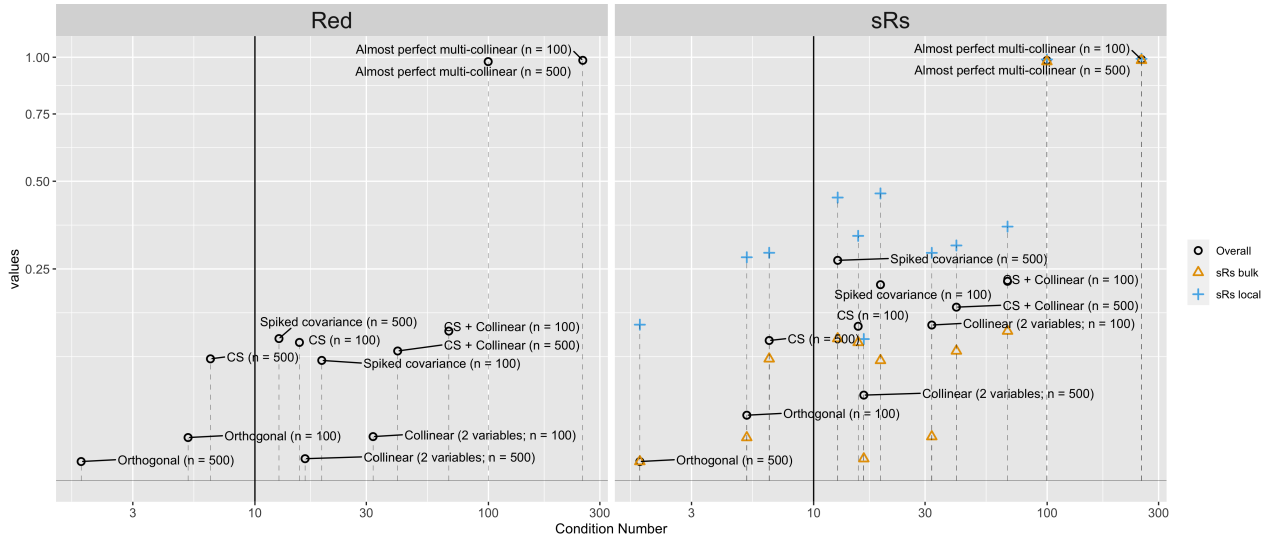
1. $\Sigma = I_p$,
2. (local) $\Sigma = \text{diag}[0.99 \times 1_2 + \sqrt{1 - 0.99^2}I_2, I_{p-2}]$,
3. (bulk) $\Sigma = \rho 1_p + (1 - \rho)I_p$ with $\rho = 0.3$ or $\rho = 0.99$,
4. (bulk and local) $\Sigma = \text{diag}[0.99 \times 1_2 + \sqrt{1 - 0.99^2}I_2, \rho 1_{p-2} + (1 - \rho)I_{p-2}]$ with $\rho = 0.3$,
5. (local) $\Sigma = LL^T + \zeta^2I_p$ with $k = 10$, $o_k^2 = 1 + \zeta^2$, and $\zeta^2 = 0.4$.

The alternative measures include *VIF*, the condition number, and the *Red* indicator. As *VIF* can only be sensibly applied when $n > p$, it was only included for comparisons in the data rich scenarios. The condition number is defined by the ratio of the largest and smallest singular values of a data matrix and describes the degree to which the matrix $X^T X$ is ill-conditioned. For the high-dimensional case, it was taken to be $\frac{d_1}{d_{n-1}}$ due to the column standardization; while for the data rich case, it was calculated as $\frac{d_1}{d_p}$. By design, the condition number captures the degree of multi-collinearity rather than the number of collinear relationships. In other words, it evaluates the worst case scenario and as a result, one perfect collinear relationship is all it takes to reach infinity, i.e. when d_p or d_{n-1} is exactly zero.

High-dimensional settings We compared the *Red* indicator and the proposed overall measure *sRs* (Equation (2.7)) to the condition number for assessing severity of multi-collinearity (Figure 2a). Unsurprisingly, the size of the condition number did not fully correspond to the severity of multi-collinearity under the impact of spurious correlations associated with high-dimensional data. In all scenarios, the *Red* indicator was identical to *BsRs*. But under $n < p$, when data matrices are necessarily under rank, and the *LsRs* component received a boost through the trailing singular values that were very close to zero. Indeed, the main advantage *sRs* had over the *Red* indicator and condition number is its sensitivity to near-collinearity $\rho = 0.99$ due to the added *LsRs* component. This contrast was expected since a global measure of “averaged linear relationship” might be less sensitive to local collinearity, for example, when two variables are near collinear. Given a fixed sample size, *Red* ranked the compound symmetry structure to be less severely multi-collinear than the spiked covariance structure as opposed to the other way around for *sRs*. This is because *sRs* puts more weight on the bulk of correlations through their contributions to d_1 , as well as locally strong correlation through their influences on d_p or d_{n-1} . In the case of a low rank structure, the larger *sRs* was due to the strong regional (between local and bulk) correlations, which contributed to the first a few leading singular values. In contrast, multi-collinearity under a compound symmetry structure has only one leading singular value, and thus the advantage of *sRs* was less pronounced.



(a) High-dimensional settings



(b) Data rich settings

Figure 2: Measuring overall severity of multi-collinearity using condition number, *Red* indicator and *sRs*. The vertical line marks the condition number cut-off at 10 to suggest presence of possible multi-collinearity.

Data rich settings When $n > p$, sR_s showed better agreement with the commonly used condition number than Red as reflected by points being closer to the line of reference, especially for the detection of two collinear variables (Figure 2b). On the other hand, Red was unable distinguish the scenarios of a compound symmetric covariance and that combined with two near collinear variables. Notice that a compound symmetric covariance with $\rho = 0.3$ is not considered to have a concerning level of multi-collinearity as these are p very weak collinear relationships, all of the same size.

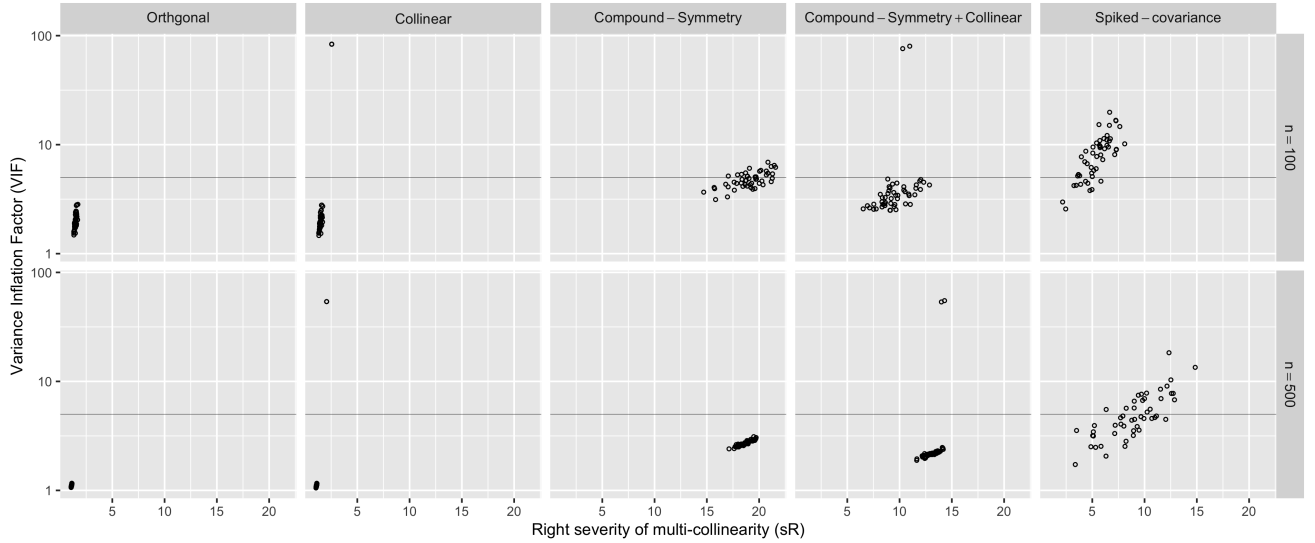


Figure 3: A scatterplot of VIF_j and sR_j under data rich settings. The horizontal line indicates a detection threshold of 5 for VIF_j .

In terms of individualized measures, though VIF_j and sR_j were designed to capture slightly different features of data, they did correlate to some extent, especially when sample size is large ($n = 500$; Figure 3). As discussed in Supplementary Section 6, the numerical difference between the two measures is due to the joint correlation structure in the remaining $p - 1$ variables. The results in fact suggested these two measures are complementary to each other. Given the same VIF_j value by varying the remaining $p - 1$ variables, the pairwise correlation of j th variable with each of the $p - 1$ variables can vary. For example, two variables having the same VIF_j value means they can be equally explained by the other $p - 1$ variables. At the same time, the same two variables could have similar or very different sR_j values, with a larger sR_j suggesting the involvement of a larger number of individually weak relationships and a smaller sR_j suggesting the involvement of a few, but stronger relationships.

4 Application to the 1000 Genomes Project Data

The population genetics equivalent of multi-collinearity is linkage disequilibrium (LD), reflecting correlation between different genetic markers. For any pair of bi-allelic markers, the LD can be quantified by the squared Pearson's correlation coefficient. LD can be interpreted at the genome-wide scale to reflect population history, breeding system and the geographic subdivision within human populations [Slatkin, 2008]. At the same time, it can be viewed at a regional level indicating influences from selection, mutation and gene conversion [Slatkin, 2008]. Thus, as the number of genetic markers involved increased, the large numbers of pairwise Pearson's correlation coefficients make the studying of LD pattern over genomic regions of arbitrary size a challenging task.

The 1000 Genomes Project [1000 Genomes Project Consortium and others, 2015] is a well-established reference for genetic variations and contains samples from several continental and sub-region populations. We applied the individual-valued uBVA and sR_s , along with LsR_s and BsR_s , measures to understand the severity of multi-collinearity within genetically homogeneous populations, as well as contrasting these measures across populations. The univariate sR_j allows the comparison at each genetic marker, while the overall measures can be used to inform the overall burden of multi-collinearity.

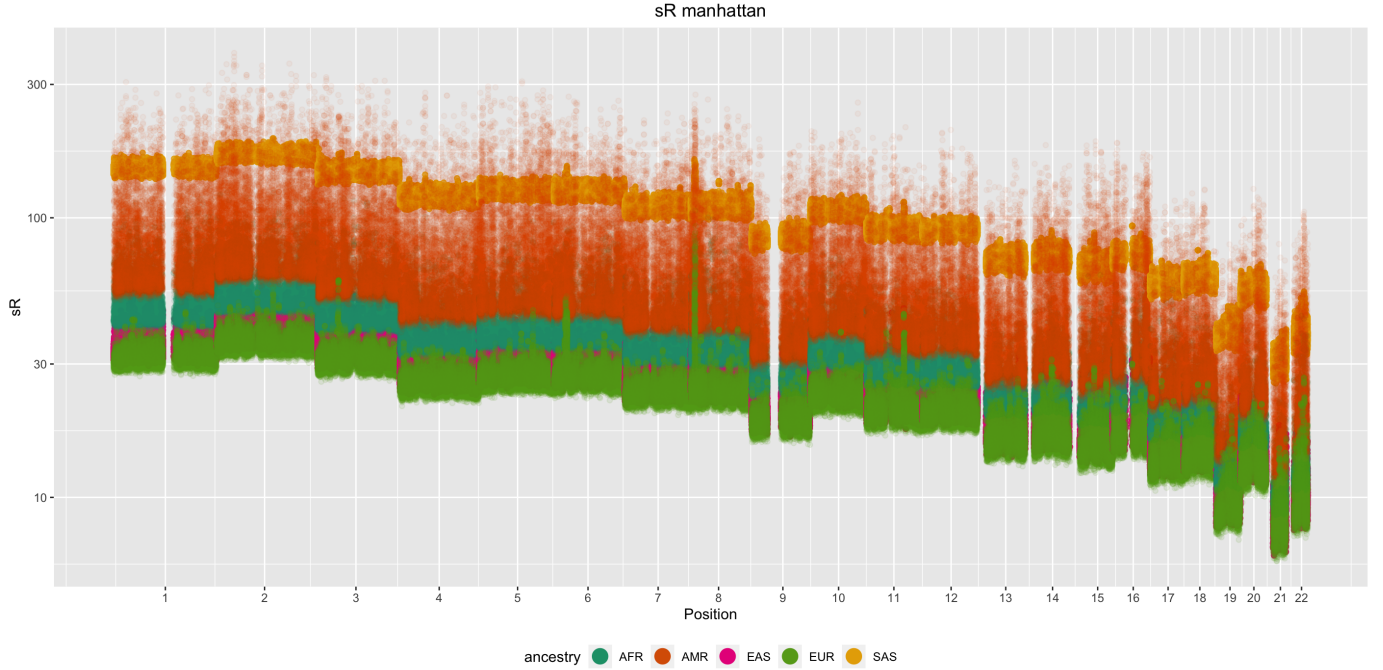


Figure 4: A Manhattan type plot for $\{sR_j\}$ as a function of the genomic location within each chromosome.

4.1 Data information and quality controls

Standard quality controls on the genotype data are outlined in Roslin et al. [2016] and the data are publicly available (<http://www.tcag.ca/tools/1000genomes.html>). This set of data contains individuals from Africa (AFR; $n = 353$), East Asia (EAS; $n = 480$), Europe (EUR; $n = 522$), South Asia (SAS; $n = 100$), and the Latin America (AMR; $n = 269$). The analyses were restricted to bi-allelic markers on autosomes. For each continental population, we applied additional data filtering steps to exclude single nucleotide polymorphisms (SNPs) with minor allele frequency (MAF) less than 0.01, with any missingness, and Hardy-Weinberg Equilibrium p -value $< 1E-5$. To harmonize the analysis in the combined sample, we retained only SNPs present in all continental populations, leaving 193,744 SNPs in the analysis, representing 20%-50% of the SNPs originally available in each population. The genomic coordinates are based on the GRCh37/hg19 build. As a control step, we produced the first two genetic principal components using the subset of overlapping SNPs, and confirmed that they are sufficient to stratify samples at the continental and sub-population level (Figure S1).

4.2 Chromosome specific patterns of multi-collinearity

The uBVA measures (i.e. $\{sR_j\}$) were calculated for each chromosome separately and presented in a similar manner to a Manhattan plot (Figure 4), typical for genome-wide applications. We expected them to roughly follow the chromosome size (number of SNPs), but with varying peaks and valleys highlighting specific regions of high/low local multi-collinearity. Interestingly, there are a large number of visible peaks in the Europeans, only some of them are shared with other populations, in particular those well-known long range LD regions at chromosome 6, 8 and 11 [Price et al., 2008] with slight differences in the exact location for different populations. For example, the region identified on chromosome 6 overlaps with the human leukocyte antigen (HLA) region. In Europeans, the peak region ranged from 25.9MB to 32.7MB, similar to the 26.4MB to 33.5MB in East Asians, but was much shorter in South Asians, only between 31.0MB to 32.3MB.

In general, East Asian, European and South Asian have sporadic long-range LD regions, represented by the occasional peaks in Figure 4, while populations in Latin America and Africa seemed to have more complex patterns of long and short range LD, corroborating the findings in Park [2019].

We observed two types of collective patterns of $\{sR_j\}$ across chromosomes and populations: those from populations in East Asia, Europe, and South Asian can be classified as being roughly symmetric (Figures S10, S4, and S6) and those from Africa and Latin America tended to have heavier tails for most chromosomes (Figures S2, S8). The shift

in the overall distribution should not be heavily influenced by outliers, such as the presence of a few long range LDs regions or strong LD blocks. Rather, considering the high-level of admixture in these populations, we hypothesized that these were probably the result of enriched genetic diversity manifested as a handful of large eigenvalues within each population (Figures S3, S11, S5, S9, and S7).

4.3 Genome-wide summaries of multi-collinearity

We then examined the overall level of multi-collinearity using genome-wide data (all 193,744 SNPs) and the results suggested the majority of multi-collinearity patterns were due to local relationships rather than global. The *RED* indicator gave a slightly higher level of “averaged correlation” in South Asia population and a lower level in Europeans and East Asians. On the other hand, *sRs* offered better granularity in the type of forces driving the averaged correlation. Specifically, though both Europeans and East Asians had similar *RED* values, their *sRs* and *LsRs* values collectively suggested a stronger local multi-collinearity in Europeans than in East Asians.

	RED	sRs	LsRs	BsRs
Combined	0.01325	0.00180	0.00451	0.00018
SAS	0.02365	0.01298	0.03674	0.00056
EAS	0.01140	0.00396	0.01187	0.00013
AFR	0.01323	0.00485	0.01465	0.00017
AMR	0.01792	0.00363	0.00826	0.00032
EUR	0.01092	0.00506	0.01608	0.00012

Table 1: A genome-wide summary of multi-collinearity for each continental population and the combined samples.

5 Discussion

Originally intended for detecting multi-collinearity under $n > p$, the *Red* indicator is equally adaptable to rank the severity of multi-collinearity in high-dimensional settings ($n < p$). As a measure of “averaged” correlation in the data, *Red* is sensitive to multi-collinearity that severely affects a large number of variables, but tends to ignore strong local relationships in the presence of moderate bulk relationships. Indeed, unlike *sRs*, *Red* does not have a mechanism to distinguish local and bulk relationships. On the other hand, the condition number is perhaps more specific to detect ill-posed problems as it is directly related to the numerical accuracy of the inverse of $X^T X$. Though these measures are sometimes useful as indicators of the overall multi-collinearity, they fall short in generating variable-specific information. As compared to sR_j , the individual-valued VIF_j can also identify specific variables involved in ill-conditioned problems and is capable of harvesting both local and global linear relationships, but can only be applied when $n < p$. In conclusion, the proposed *sRs*, *BsRs* and *LsRs*, combined with $\{sR_j\}$ are recommended as measures of multi-collinearity in high-dimensional settings.

We want to highlight some potential improvements that are of interest for future research work. Firstly, sR_j are empirical measures and a natural next step is to leverage theoretical results from random matrix theory to further derive their statistical properties. Secondly, it would be of interest to construct two-sample or multiple-sample statistical tests for quantities such as *sRs*, *BsRs* and *LsRs*, thus enabling a formal statistical comparison of the severity and sources of multi-collinearity. Finally, though the application to autosomal markers yielded insightful results, the same might not translate to the X-chromosome due to differences in the number of chromosomal copies between sexes. One of the complications is that since females carry two copies and males carry only one copy of the X-chromosome, the multi-collinearity measures derived from the observed data are expected to vary with respect to the sex ratios. As a result, though the measures are still valid in the sense that they can be computed and reflect the observed severity of multi-collinearity, they cannot be reliably used to compare LD patterns between samples.

It is worth noting that similar measures to sR_j have been proposed in genetic applications: *LDadj* was used in the construction of polygenic risk scores (PRS) for prediction [Pare et al., 2016, 2017], and *LDscore* was used to demonstrate the polygenicity of a trait, such as in LD-score regression [Bulik-Sullivan et al., 2015]. Both are in fact truncated versions of the sR_j and are denoted by the sum of squared Pearson’s correlation coefficients:

$$LDadj_{(j)} = \sum_{j'=j-t}^{j+t} r_{j'j}^2, \quad (5.1)$$

and

$$LDscore_{(j)} = \sum_{j'=j-t}^{j+t} r_{j'j}^2 - \frac{1 - r_{j'j}^2}{n-2}, \quad (5.2)$$

where $LDscore$ has an additional term such that each squared Pearson's correlation remains unbiased (under $n > t$). The value of t is defined by assuming the neighbouring t genetic variants up- and down-stream are sufficient to capture the local LD (or covariance) structure, thus the choice is subjective. A window of radius 1 centiMorgan around the index variant was recommended [Bulik-Sullivan et al., 2015]. Contrary to uBVA, $LDadj$ or $LDscore$ do not intend to capture the systematic effect, but only the local effect of multi-collinearity. Consequently, these truncated measures are restricted to analyses within a homogeneous population and are not tailored for comparisons across samples of distinct populations; further, since the truncation occurs through a rolling window, the measures are not directly comparable from variable to variable.

6 Concluding remarks

Our multi-collinearity measures $\{sR_j\}$ offer an alternative univariate perspective to visualize multi-collinearity patterns. They also enable the construction of a high-level summary measure sRs that sheds light on the sources of multi-collinearity through the relative contribution from $LsRs$ and $BsRs$, which can inform the choice of an appropriate data learning strategy. The fact that these can be applied regardless of data dimensions is an attractive feature in high-dimensional data applications. Besides providing a visual inspection and numerical summary of multi-collinearity in high-dimensions, the proposed measures are amendable to various downstream analyses and potential applications, for example, as informative shrinkage weights to construct high-dimensional estimators. Finally, the simplicity in their construction also enables convenient data sharing for open science research.

Acknowledgement

The authors would like to acknowledge Professors Dehan Kong and Stanislav Volgushev for a critical reading and their insightful comments on the early versions of the paper. The authors are grateful to Drs. Michael R. Chong and Nicholas Perrot for lengthy discussions and their constructive comments on the genetic applications.

Funding Information

This research is funded by the Natural Sciences and Engineering Research Council of Canada (NSERC), the Department of Statistical Sciences at University of Toronto, and the Canadian Institutes of Health Research (CIHR).

Supplementary Materials

Proofs

Proof of property 2.1

Proof. : Since XX^TXX^T is a square matrix with non-negative eigenvalues d_1^4, \dots, d_{n-1}^4 , the trace is simply the sum of eigenvalues:

$$\text{tr}(XX^TXX^T) = \sum_{i'=1}^{n-1} d_{i'}^4.$$

It then follows from the cyclic property of trace that:

$$\sum_{j=1}^p SR_j = \text{tr}(X^TXX^TX) = \text{tr}(XX^TXX^T) = \text{tr}(UD^4U^T) = \sum_{i=1}^n SL_i.$$

Proof of property 2.2

Proof. :

$$\text{diag}[\text{cor}(X)^2]_j = \text{diag} \left[\frac{X^TXX^TX}{(n-1)^2} \right]_j = \frac{SR_j}{(n-1)^2},$$

and

$$\text{diag}[\text{cor}(X)^2]_j = \sum_{j'=1}^p r_{jj'}^2.$$

Proof of property 2.2

Proof. : Following the Cauchy-Schwarz inequality, the lower bound is given by:

$$\begin{aligned} SR_j &= \sum_{i'=1}^{n-1} v_{ji'}^2 d_{i'}^4 = \sum_{i'=1}^{n-1} \frac{(v_{ji'}^2 d_{i'}^2)^2}{v_{ji'}^2} \\ &\geq \frac{(\sum_{i'=1}^{n-1} v_{ji'}^2 d_{i'}^2)^2}{\sum_{i'=1}^{n-1} v_{ji'}^2} \\ &= \frac{(n-1)^2}{\sum_{i'=1}^{n-1} v_{ji'}^2} \geq (n-1)^2, \end{aligned}$$

while the upper bound is:

$$\begin{aligned} SR_j &= \sum_{i'=1}^{n-1} v_{ji'}^2 d_{i'}^4 \\ &\leq d_1^2 \sum_{i'=1}^{n-1} v_{ji'}^2 d_{i'}^2 \\ &= d_1^2 (n-1). \end{aligned}$$

Proof of Lemma 2.1

Proof. Since SR_j is simply the j th diagonal element of $X^T X X^T X$, we approach this by calculating the expected value of $SR_j = e_j^T X^T X X^T X e_j$, where $e_j = (0, \dots, 0, 1, 0, \dots, 0) \in \mathbb{R}^p$ is a standard basis vector with value 1 at the j th place. Further, it follows that $(n-1)\hat{\Sigma} = X^T X \sim \mathcal{W}_p(\Sigma, n)$ has a Wishart distribution with parameters Σ and degrees of freedom n .

Following Proposition S1 of [Dicker, 2014], where explicit expressions for the expectation of moments of a Wishart random matrix were derived, it is easy to write down the expectation of SR_j as:

$$\begin{aligned} E(e_j^T X^T X X^T X e_j) &= p(n-1) \frac{\text{tr}(\Sigma_p)}{p} e_j^T \Sigma_p e_j + n(n-1) e_j^T \Sigma_p \Sigma_p e_j \\ &= (n-1)(\Sigma_p)_{jj} \text{tr}(\Sigma_p) + n(n-1)(\Sigma_p)_{.j}^T (\Sigma_p)_{.j}. \end{aligned}$$

The expectation can be further simplified if the true covariance Σ has diagonal elements 1:

$$E(SR_j) = (n-1)p + n(n-1)\Sigma_j^T \Sigma_j.$$

□

Relationship with existing measures of multi-collinearity

Since measures are often derived from sample eigenvalues, which are closely related to singular values, here we reveal the relationship between proposed and existing measures of multi-collinearity.

The Red indicator Both the *Red* indicator [Kovács et al., 2005] and sR_j can be used without dimension restrictions and it turns out the two are closely related:

$$\text{Red} = \sqrt{\frac{\text{tr}[X^T X X^T X - (n-1)^2 I_p]}{p(p-1)(n-1)^2}} = \sqrt{\frac{\sum_{j=1}^p sR_j - p}{p(p-1)}},$$

where $\text{Red} \in [0, 1]$ and $sR_j \in [1, p]$ following Equation (2.3). It is regarded as a global measure of average correlation in the data over all pairwise variables or the proportion of redundant information, with values closer to 1 indicating

a large number of near or perfect multi-collinearity relationships and values closer to 0 indicating little evidence of multi-collinearity. Given how *Red* is defined, the authors did not provide a recommended threshold at which a concerning level of multi-collinearity is present.

In relation to *Red*, sR_j can be seen as its individual-level counterpart and is potentially more useful for contrasting variables for their relative involvement in multi-collinearity. It should be emphasized that individual sR_j values alone cannot distinguish between the “bulk weak” and “local strong” scenarios as the same sR_j value could be given by many weak relationships or a few strong relationships. In reality, the ambiguity also remains for *Red* indicator values that are closer to the middle. For example, a *Red* value of 0.4 can be achieved by either a large number of weak collinear relationships or a small number of perfect or near collinear relationships, with the latter having a bigger impact on matrix solutions to linear regression problems.

Variance Inflation Factor (VIF) Though the *VIF* is restricted to the setting of $n > p$, it is still of interest to compare sR_j and *VIF*_{*j*} on an equal footing as individual-valued measures. Note that when $n > p$, components of the SVD of X have different dimensions: $U \in \mathbb{R}^{n \times p}$, $V \in \mathbb{R}^{p \times p}$, and $D = \text{diag}[d_1, \dots, d_p] \in \mathbb{R}^{p \times p}$. In this case, d_p does not equal to 0 following the column-wise mean and variance standardization. It should be noted that *VIF*_{*j*} is only suitable when the data matrix is full rank, while sR_j can be calculated without such restriction.

The *VIF* of the *j*th predictor can be expressed as:

$$\begin{aligned} VIF_j &= \frac{1}{1 - R_j^2} \\ &= \frac{x_j^T x_j}{x_j^T x_j - x_j^T X_{-j} (X_{-j}^T X_{-j})^{-1} X_{-j}^T x_j} \\ &= \frac{1}{1 - (n-1) b_{-j}^T (X_{-j}^T X_{-j})^{-1} b_{-j}}, \end{aligned} \quad (6.1)$$

where x_j denotes the *j*th column of X , X_{-j} the data matrix with *j*th column removed, and $b_{-j} = \frac{1}{n-1} X_{-j}^T x_j$ the vectorized univariate regression coefficients estimated between the *j*th variable and each of the other $p-1$ variables. Using the same notation, the multivariate regression coefficients estimated using the *j*th variable as the response and the other $p-1$ variables as the predictors can be expressed as $(n-1)(X_{-j}^T X_{-j})^{-1} b_{-j}$.

The proposed measure sR_j can be similarly expressed:

$$\begin{aligned} sR_j &= \sum_{j'=1}^p r_{jj'}^2 \\ &= \left[1 + \sum_{j' \neq j} \left(\frac{1}{n-1} x_{j'}^T x_j \right)^2 \right] \\ &= (1 + b_{-j}^T b_{-j}). \end{aligned} \quad (6.2)$$

Both *VIF*_{*j*} and sR_j are driven by b_{-j} , with the main difference being how $b_{-j}^T b_{-j}$ is weighted. Note that as $(X_{-j}^T X_{-j})^{-1}$ is capable of simultaneously modelling relationship among the other $p-1$ variables, *VIF*_{*j*} is expected to be more sensitive than sR_j at recognizing multi-collinearity that involves a large number of variables as each element of $b_{-j}^T b_{-j}$ merely describes the strength of a bivariate relationship. From the alternative expression of sR_j according to the definition via the singular values, we obtain

$$sR_j = (n-1)^{-2} \sum_{i'=1}^p v_{ji'}^2 d_{i'}^4 = d_1^2 (n-1)^{-2} \left[\sum_{i'=1}^p (v_{ji'}^2 d_{i'}^2) \frac{d_{i'}^2}{d_1^2} \right]. \quad (6.3)$$

Though each $d_{i'}$ is weighted towards sR_j , the collective behaviour of sR_j will be influenced by a large d_1 and therefore captures information in the condition indices $\left\{ \frac{d_1}{d_{i'}} \right\}_{i'=1, \dots, p}$.

An important aspect is the detection of variables involved in multi-collinearity, which often requires a hard detection threshold. For the individual sR_j , suppose the data matrix is column standardized, one possible threshold for sR_j could be due to property 2.2 combined with an approximated distribution for the sample Pearson’s correlation coefficient given in Stuart et al. [1994]:

$$r = \frac{t}{\sqrt{n-2+t^2}},$$

where t is a random variable following Student's t -distribution with degrees of freedom $n - 2$. This results holds approximately for large enough n and the pairs of variables are assumed to be uncorrelated. It can be shown that r^2 then follows a beta distribution with shape parameters $1/2$ and $(n - 2)/2$, and $E(r^2) = (n - 1)^{-1}$. Thus, a possible threshold for departure from orthogonal columns using sR_j could be $\frac{p-1}{n-1} + 1$ by summing up the $p - 1$ expected values of squared sample Pearson's correlation coefficients assuming the true pairwise correlation is zero throughout.

Connection to the effective sample size and effective number of variables

Typically, in a regression, correlated samples do not change mean estimation, but rather influence inference through increased variance. As a result, the same estimator under correlated samples should have a variance adjusted for the effective sample size. For correlated variables, an analogous concept is the effective number of variables, which serves as an upper bound for the effective degrees of freedom of a model (usually defined as the trace of the hat matrix connecting the response to its fitted values, e.g. $H = X(X^T X)^{-1} X^T$, for OLS regression).

Here we focus on the effective number of variables and the effective sample size, without referencing a model fitting procedure, and show that the proposed measure of multi-collinearity can be used to inform the maximum possible values for both. As a result of the dual (i.e. column and row) perspectives on a data matrix X , the same technique can be applied to either X or X^T provided that the respective columns or rows are standardized to have mean 0 and variance 1.

Given a row standardized X and $n > p$, the effective sample size as determined by the left severity measure is at most:

$$\sum_{i=1}^n \frac{1}{sL_i} \leq \sum_{i=1}^n \sum_{i'=1}^p u_{ii'}^2 = p.$$

Analogously, given a column standardized X and $n < p$, $\sum_{j=1}^p \frac{1}{sR_j}$ can be considered the effective number of variables. Further, it can be shown that $\sum_{j=1}^p \frac{1}{sR_j}$ is at most $n - 1$ following property 2.3. To see this, for each j :

$$\frac{1}{sR_j} \leq \sum_{i'=1}^{n-1} v_{ji'}^2,$$

which suggests that:

$$\sum_{j=1}^p \frac{1}{sR_j} \leq \sum_{j=1}^p \sum_{i'=1}^{n-1} v_{ji'}^2 = n - 1.$$

Since $\frac{1}{sR_j}$ is a constant between $1/p$ and 1, it can be viewed as the amount of non-redundant information in a variable prior to model selection. Consider the extreme case when all variables were truly uncorrelated, but under the impact of spurious correlation in high dimensions, the maximum degrees of freedom becomes $\min(n, p) - 1 = n - 1$, meaning every variable is equally important prior to model selection. The opposite scenario is when all variables completely correlate with each other, the maximum degrees of freedom reduce to 1. Though each variable is equally important, their relative importance would be scaled by $\frac{1}{p}$, meaning the model can include any one of the variables.

However, these two concepts are really two sides of the same coin arising from the execution of a row or column standardization. For convenience, briefly consider a doubly centred ($\sum_{i=1}^n x_{ij} = \sum_{j=1}^p x_{ij} = 0$) and doubly standardized ($\sum_{i=1}^n x_{ij}^2 = n - 1$ and $\sum_{j=1}^p x_{ij}^2 = p - 1$) data matrix X .

Suppose $n > p$, assume a multivariate normal model for each row of X with independent samples:

$$x_i \stackrel{\text{iid}}{\sim} \mathcal{N}(0, \Sigma), \quad i = 1, 2, \dots, n,$$

where $\Sigma \in \mathbb{R}^{p \times p}$. With the means removed, it follows that $\hat{\Sigma} = \frac{1}{n} X^T X$ has a scaled Wishart distribution with mean and variance

$$E(\hat{\Sigma}) = \Sigma \quad \text{and} \quad \text{Var}(\hat{\Sigma}) = \frac{1}{n} \Sigma^{(2)},$$

where $\Sigma_{jk, lh}^{(2)} = \Sigma_{jl}^{(2)} \Sigma_{kh}^{(2)} + \Sigma_{jh}^{(2)} \Sigma_{kl}^{(2)}$ and $\Sigma^{(2)} \in \mathbb{R}^{p^2 \times p^2}$.

Similarly, suppose $n < p$, a multivariate normal model can be assumed for each column of X with independent variables:

$$x_j \stackrel{\text{iid}}{\sim} \mathcal{N}(0, \Phi), \quad j = 1, 2, \dots, p,$$

where $\Phi \in \mathbb{R}^{n \times n}$. It follows that $\hat{\Phi} = \frac{1}{p} X X^T$ has a scaled Wishart distribution with mean and variance

$$E(\hat{\Phi}) = \Sigma \quad \text{and} \quad \text{Var}(\hat{\Phi}) = \frac{1}{p} \Phi^{(2)},$$

where $\Phi_{jk, lh}^{(2)} = \Phi_{jl}^{(2)} \Phi_{kh}^{(2)} + \Phi_{jh}^{(2)} \Phi_{kl}^{(2)}$ and $\Phi^{(2)} \in \mathbb{R}^{n^2 \times n^2}$.

Following Theorem 8.4 of Efron [2012], when rows of X are not independent and $n > p$, the effective sample size n_{eff} is defined by

$$n_{\text{eff}} = \frac{n}{1 + (n-1) \left[\frac{n \sum_{i'=1}^p d_{i'}^4}{n(n-1)p^2} - \frac{1}{n-1} \right]} = \frac{n^2 p^2}{\sum_{i'=1}^p d_{i'}^4} = \frac{n^2}{\sum_{i=1}^n sL_i}. \quad (6.4)$$

In comparison, when columns of X are not independent and $n < p$, the effective number of variables (p_{eff}) is defined by

$$p_{\text{eff}} = \frac{p}{1 + (p-1) \left[\frac{p \sum_{i=1}^{n-1} d_i^4}{n^2 p(p-1)} - \frac{1}{p-1} \right]} = \frac{n^2 p^2}{\sum_{i=1}^{n-1} d_i^4} = \frac{p^2}{\sum_{j=1}^p sR_j}. \quad (6.5)$$

The inequality of arithmetic and geometric means implies

$$\frac{p^2}{\sum_{j=1}^p sR_j} \leq \sum_{j=1}^p \frac{1}{sR_j},$$

and

$$\frac{n^2}{\sum_{i=1}^n sL_i} \leq \sum_{i=1}^n \frac{1}{sL_i},$$

which shows that $\sum_{j=1}^p \frac{1}{sR_j}$ and $\sum_{i=1}^n \frac{1}{sL_i}$ are indeed the maximum possible values for the effective number of variables and effective sample size, respectively.

Supplementary Figures

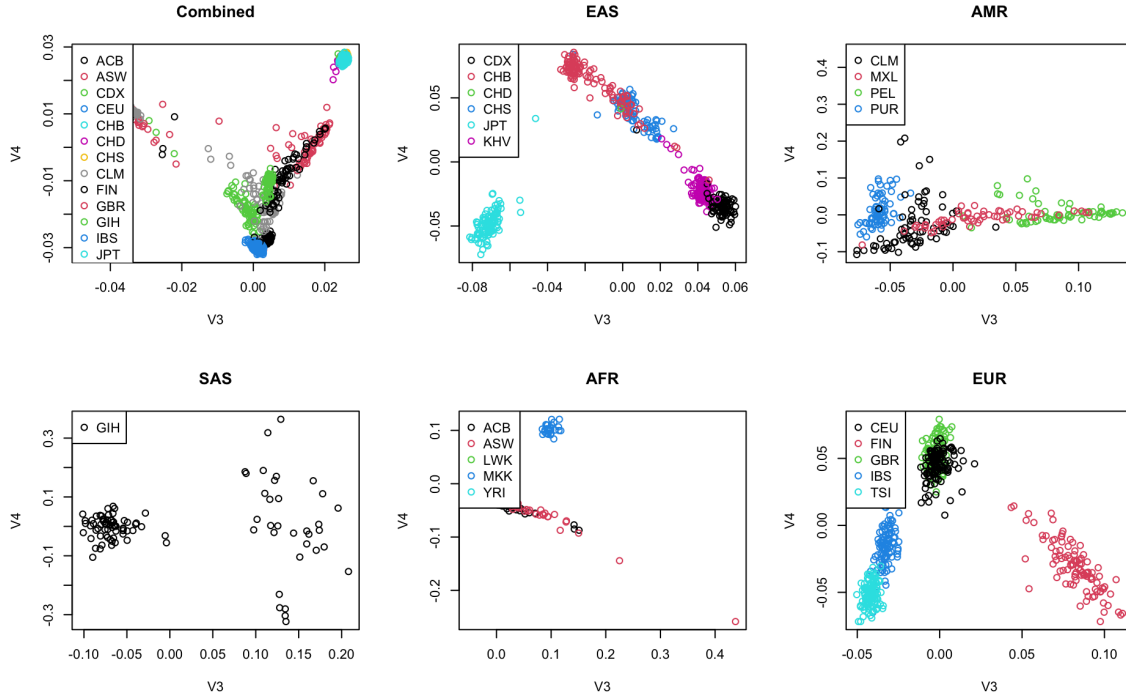


Figure S1: Scatterplots of the first genetic principal components for the combined and each continental populations.

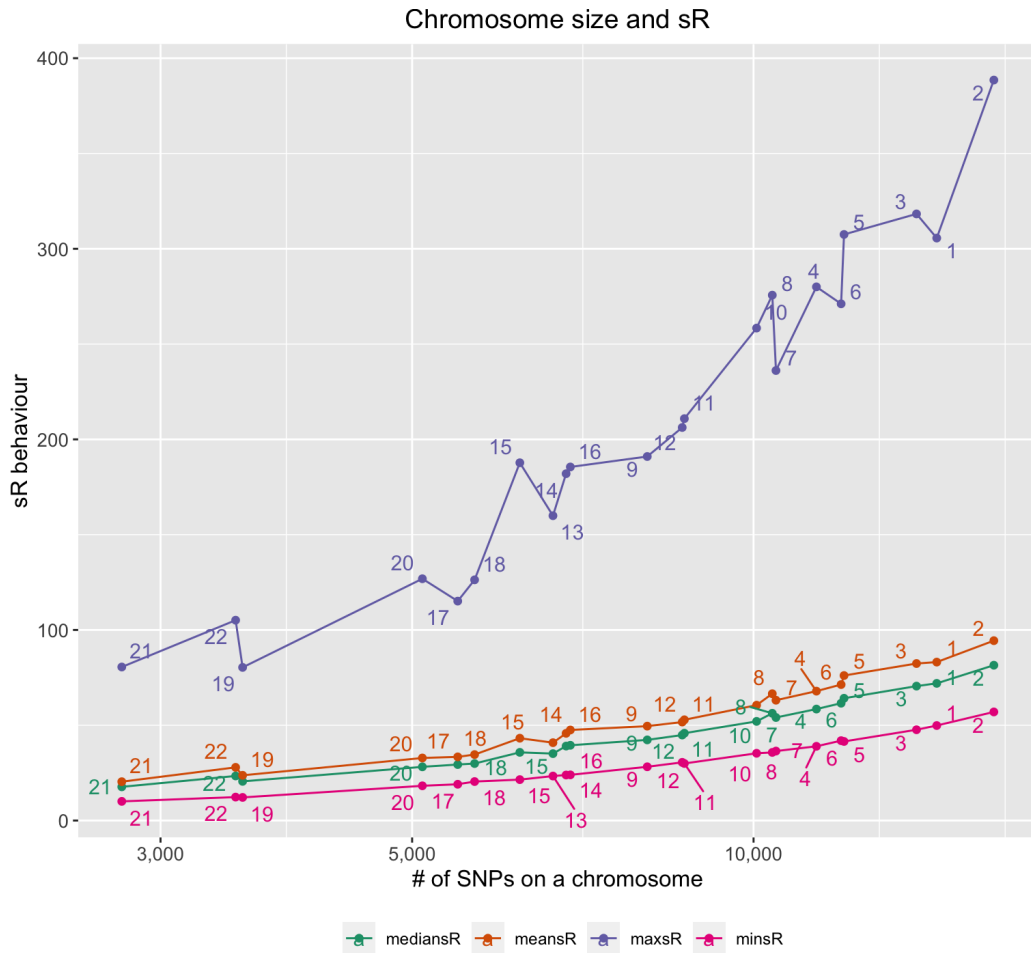


Figure S2: A summary of multi-collinearity as a function of chromosome size for populations in America.

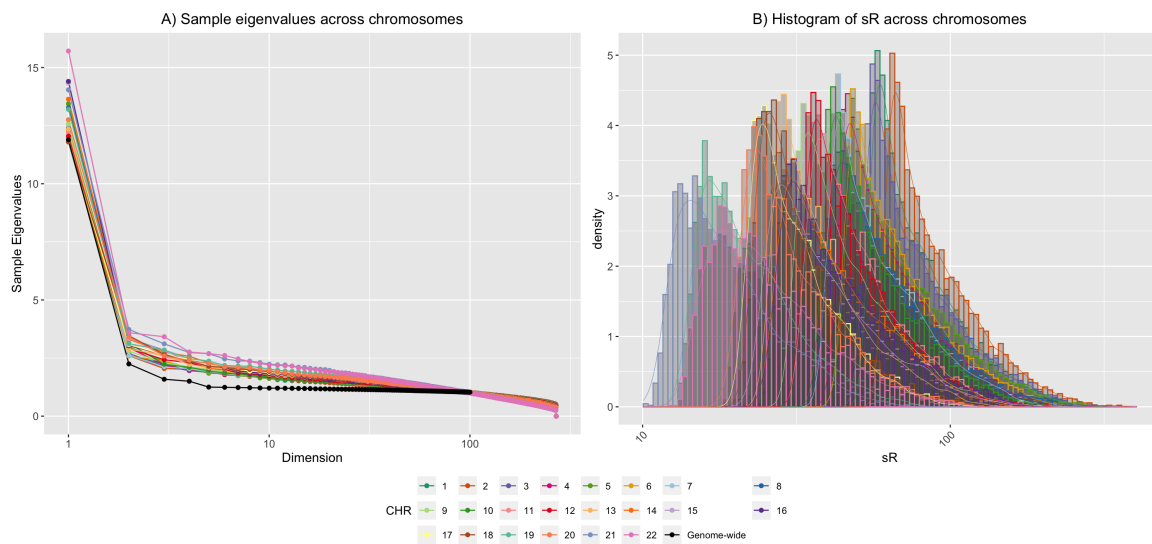


Figure S3: Patterns of multi-collinearity measured by $\{sR_j\}_j$ in America.

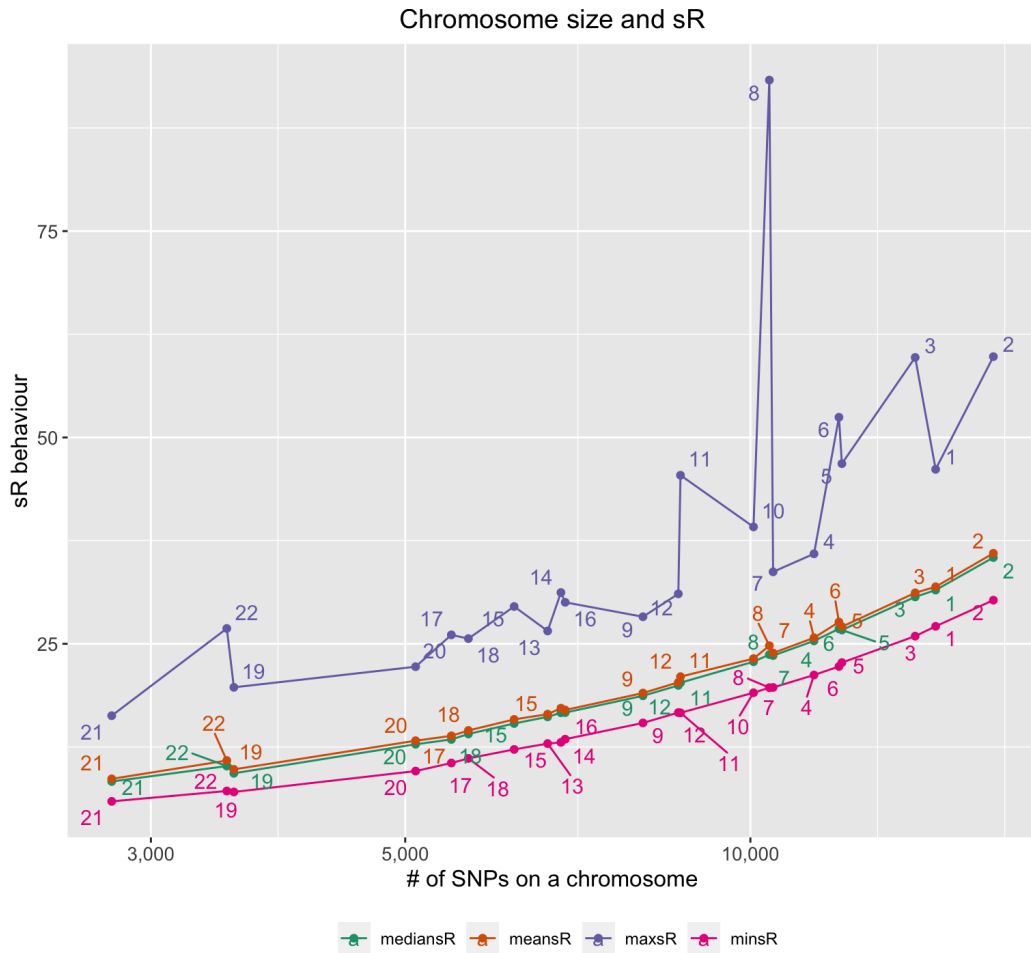


Figure S4: A summary of multi-collinearity as a function of chromosome size for populations in Europe.

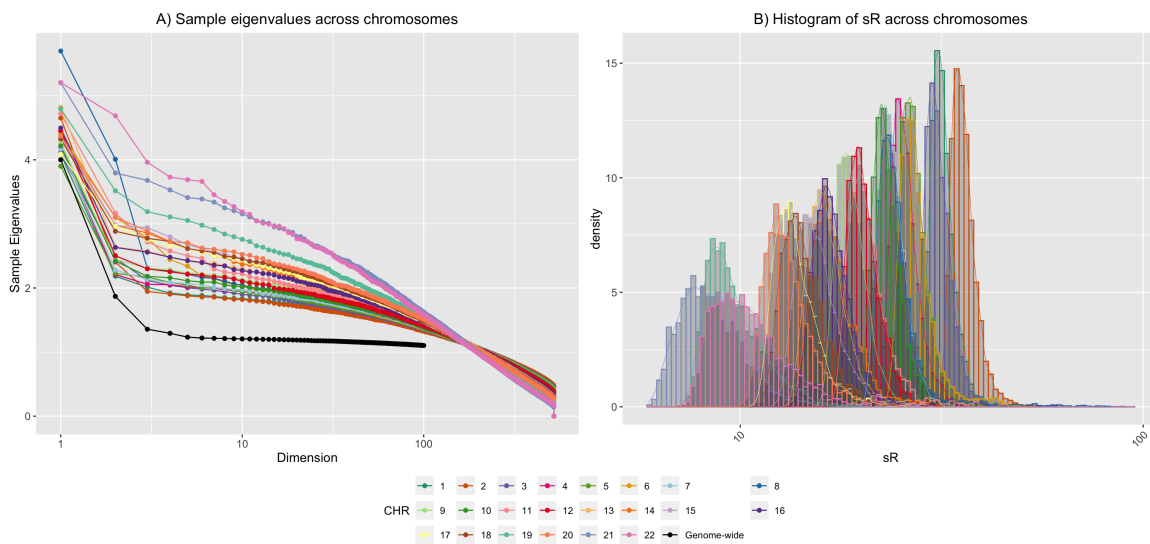


Figure S5: Patterns of multi-collinearity measured by $\{sR_j\}_j$ in Europe.

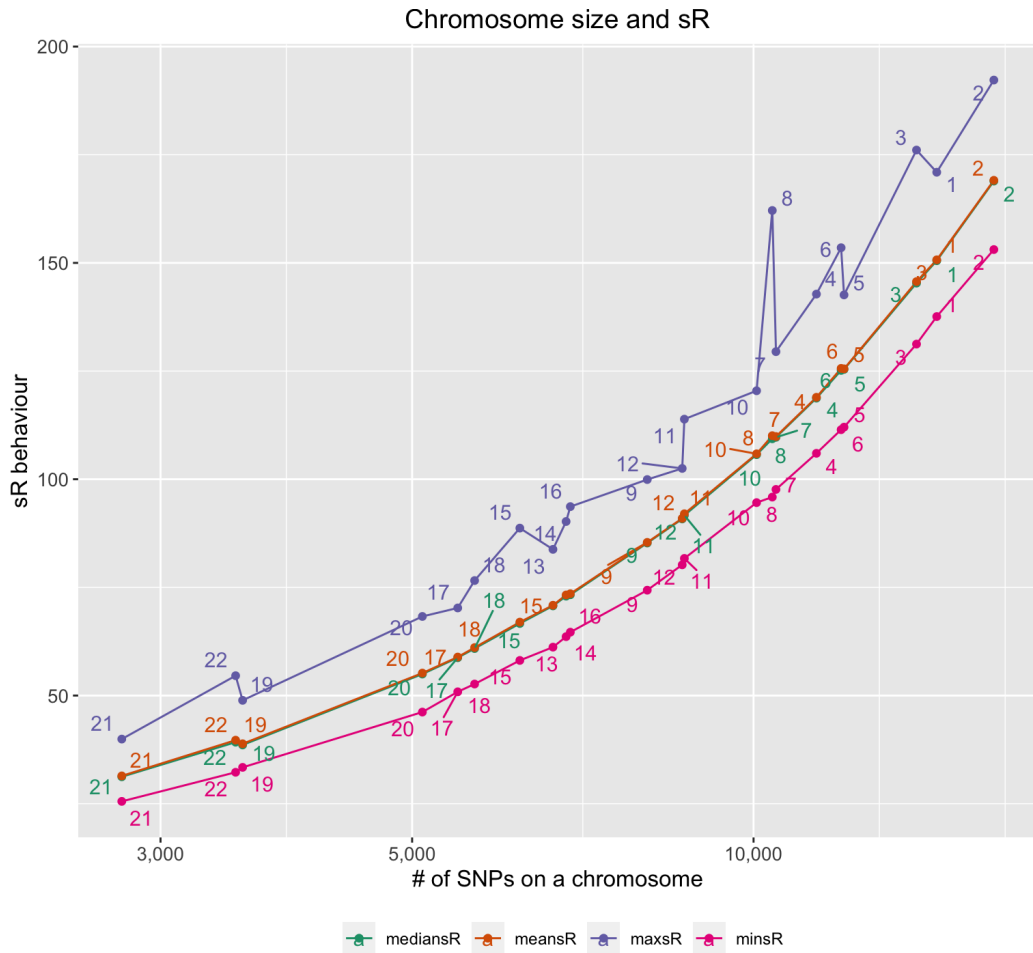


Figure S6: A summary of multi-collinearity as a function of chromosome size for populations in South Asia.

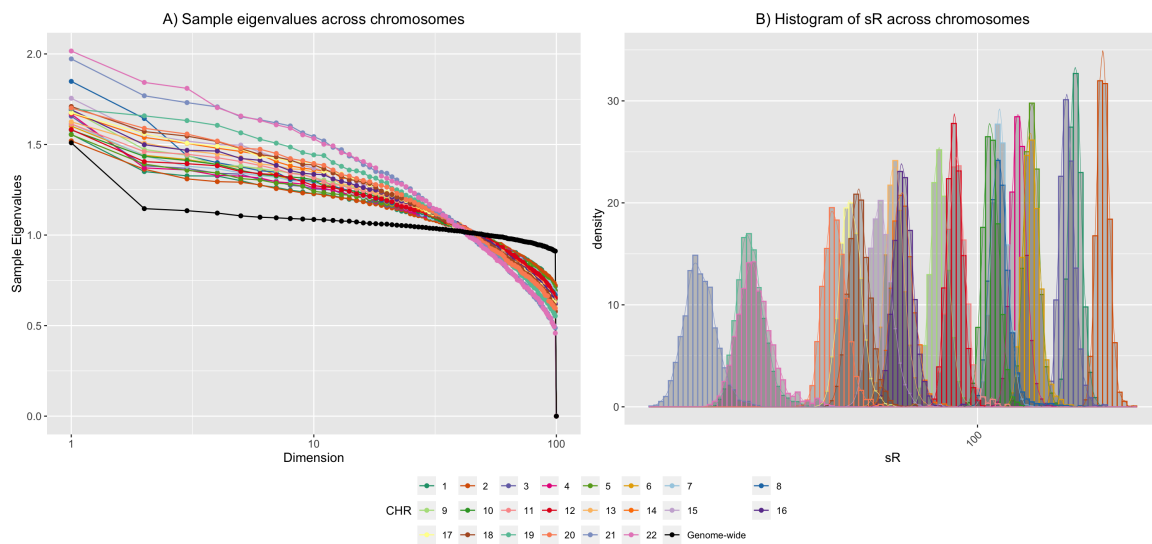


Figure S7: Patterns of multi-collinearity measured by $\{sR_j\}_j$ in South Asia.

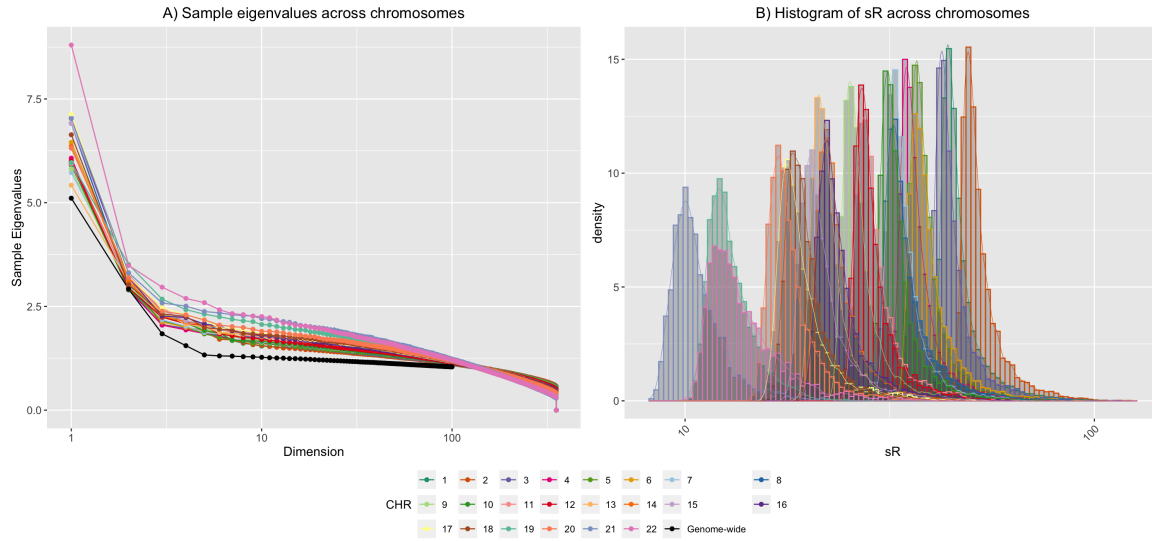


Figure S9: Patterns of multi-collinearity measured by $\{sR_j\}_j$ in Africa.

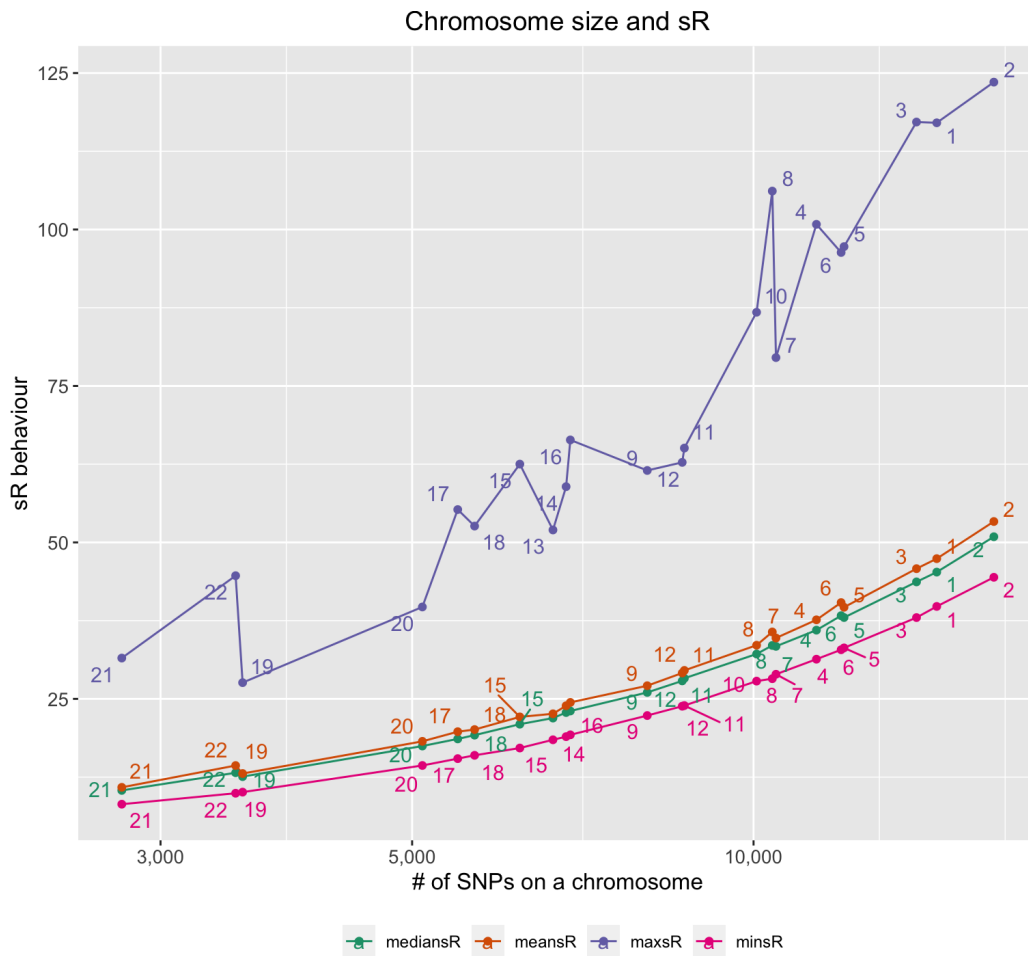


Figure S8: A summary of multi-collinearity as a function of chromosome size for populations in Africa.

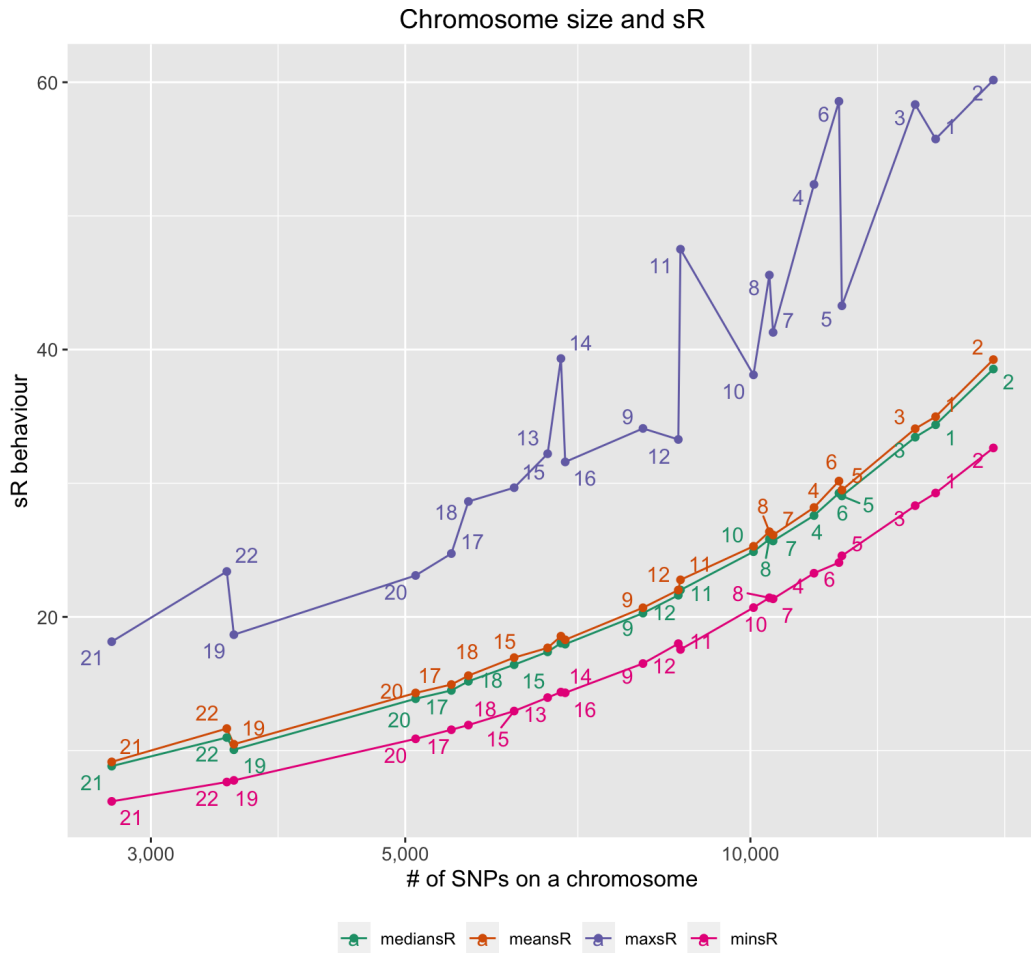


Figure S10: A summary of multi-collinearity as a function of chromosome size for populations in East Asia.

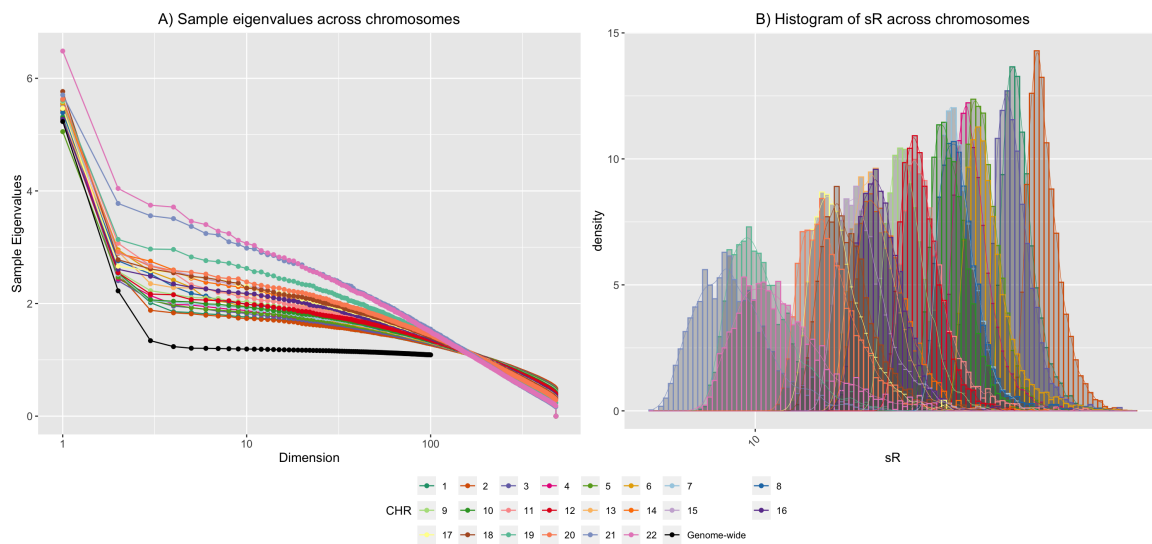


Figure S11: Patterns of multi-collinearity measured by $\{sR_j\}_j$ in East Asia.

References

- Karsten Suhre, Mark I McCarthy, and Jochen M Schwenk. Genetics meets proteomics: perspectives for large population-based studies. *Nature Reviews Genetics*, 22(1):19–37, 2021.
- David L Donoho et al. High-dimensional data analysis: The curses and blessings of dimensionality. *AMS math challenges lecture*, 1(2000):32, 2000.
- Jianqing Fan and Jinchi Lv. Sure independence screening for ultrahigh dimensional feature space. *Journal of the Royal Statistical Society: Series B (Statistical Methodology)*, 70(5):849–911, 2008.
- Larry Wasserman and Kathryn Roeder. High dimensional variable selection. *Annals of statistics*, 37(5A):2178, 2009.
- Edward I George. The variable selection problem. *Journal of the American Statistical Association*, 95(452):1304–1308, 2000.
- Péter Kovács, Tibor Petres, and László Tóth. A new measure of multicollinearity in linear regression models. *International Statistical Review*, 73(3):405–412, 2005.
- Bradley Efron. Correlated z-values and the accuracy of large-scale statistical estimates. *Journal of the American Statistical Association*, 105(491):1042–1055, 2010.
- Fadil Santosa and William W Symes. Linear inversion of band-limited reflection seismograms. *SIAM Journal on Scientific and Statistical Computing*, 7(4):1307–1330, 1986.
- Robert Tibshirani. Regression shrinkage and selection via the lasso. *Journal of the Royal Statistical Society. Series B (Methodological)*, 58(1):267–288, 1996. ISSN 00359246. URL <http://www.jstor.org/stable/2346178>.
- Hui Zou and Trevor Hastie. Regularization and variable selection via the elastic net. *Journal of the Royal Statistical Society: Series B (Statistical Methodology)*, 67(2):301–320, 2005.
- Donald W Marquardt. Generalized inverses, ridge regression, biased linear estimation, and nonlinear estimation. *Technometrics*, 12(3):591–612, 1970.
- Donald E Farrar and Robert R Glauber. Multicollinearity in regression analysis: the problem revisited. *The Review of Economic and Statistics*, pages 92–107, 1967.
- David A Belsley. Conditioning diagnostics. *Wiley StatsRef: Statistics Reference Online*, 2014.
- John Fox. *Linear statistical models and related methods: With applications to social research*. John Wiley & Sons, 1984.
- José Dias Curto and José Castro Pinto. The corrected vif (cvif). *Journal of Applied Statistics*, 38(7):1499–1507, 2011.
- John R Rice. A theory of condition. *SIAM Journal on Numerical Analysis*, 3(2):287–310, 1966.
- AJ Geurts. A contribution to the theory of condition. *Numerische Mathematik*, 39(1):85–96, 1982.
- David A Belsley, Edwin Kuh, and Roy E Welsch. *Regression diagnostics: Identifying influential data and sources of collinearity*. John Wiley & Sons, 2005.
- Román Salmerón, CB García, and J García. Variance inflation factor and condition number in multiple linear regression. *Journal of Statistical Computation and Simulation*, 88(12):2365–2384, 2018.
- Kenneth N Berk. Tolerance and condition in regression computations. *Journal of the American Statistical Association*, 72(360a):863–866, 1977.
- John Fox and Georges Monette. Generalized collinearity diagnostics. *Journal of the American Statistical Association*, 87(417):178–183, 1992.
- Jianqing Fan, Shaojun Guo, and Ning Hao. Variance estimation using refitted cross-validation in ultrahigh dimensional regression. *Journal of the Royal Statistical Society: Series B (Statistical Methodology)*, 74(1):37–65, 2012.
- John Wishart. The generalised product moment distribution in samples from a normal multivariate population. *Biometrika*, pages 32–52, 1928.
- Muni S Srivastava. Singular wishart and multivariate beta distributions. *The Annals of Statistics*, 31(5):1537–1560, 2003.
- Zhidong D Bai. Methodologies in spectral analysis of large dimensional random matrices, a review. In *Advances In Statistics*, pages 174–240. World Scientific, 2008.
- Vladimir Alexandrovich Marchenko and Leonid Andreevich Pastur. Distribution of eigenvalues for some sets of random matrices. *Matematicheskii Sbornik*, 114(4):507–536, 1967.
- Montgomery Slatkin. Linkage disequilibrium—understanding the evolutionary past and mapping the medical future. *Nature Reviews Genetics*, 9(6):477–485, 2008.

- 1000 Genomes Project Consortium and others. A global reference for human genetic variation. *Nature*, 526(7571): 68–74, 2015.
- Nicole M Roslin, Li Weili, Andrew D Paterson, and Lisa J Strug. Quality control analysis of the 1000 genomes project omni2. 5 genotypes. *BioRxiv*, page 078600, 2016.
- Alkes L Price, Michael E Weale, Nick Patterson, Simon R Myers, Anna C Need, Kevin V Shianna, Dongliang Ge, Jerome I Rotter, Esther Torres, Kent D Taylor, et al. Long-range ld can confound genome scans in admixed populations. *The American Journal of Human Genetics*, 83(1):132–135, 2008.
- Leeyoung Park. Population-specific long-range linkage disequilibrium in the human genome and its influence on identifying common disease variants. *Scientific Reports*, 9(1):1–13, 2019.
- Guillaume Pare, Shihong Mao, and Wei Q Deng. A method to estimate the contribution of regional genetic associations to complex traits from summary association statistics. *Scientific Reports*, 6:27644, 2016.
- Guillaume Pare, Shihong Mao, and Wei Q Deng. A machine-learning heuristic to improve gene score prediction of polygenic traits. *Scientific Reports*, 7(1):12665, 2017.
- Brendan K Bulik-Sullivan, Po-Ru Loh, Hilary K Finucane, Stephan Ripke, Jian Yang, Nick Patterson, Mark J Daly, Alkes L Price, Benjamin M Neale, Schizophrenia Working Group of the Psychiatric Genomics Consortium, et al. Ld score regression distinguishes confounding from polygenicity in genome-wide association studies. *Nature genetics*, 47(3):291, 2015.
- Lee H Dicker. Variance estimation in high-dimensional linear models. *Biometrika*, 101(2):269–284, 2014.
- Alan Stuart, Steven Arnold, J Keith Ord, Anthony O’Hagan, and Jonathan Forster. *Kendall’s advanced theory of statistics*. Wiley, 1994.
- Bradley Efron. *Large-scale inference: empirical Bayes methods for estimation, testing, and prediction*, volume 1. Cambridge University Press, 2012.